Development of Local Feature Extraction and Reduction Schemes for Iris Biometrics

Beeren Sahu

Department of Computer Science and Engineering
National Institute of Technology Rourkela
Rourkela – 769 008, Odisha, India

Development of Local Feature Extraction and Reduction Schemes for Iris Biometrics

Thesis submitted in partial fulfillment of the

the requirements for the degree of

Master of Technology

(Research)

in

Computer Science and Engineering

by

Beeren Sahu

(Roll No. 612CS6003)

under the guidance of

Dr. Pankaj K. Sa

&

Prof. Banshidhar Majhi

Department of Computer Science and Engineering
National Institute of Technology Rourkela
Rourkela-769 008, Odisha, India

Department of Computer Science and Engineering
National Institute of Technology Rourkela
Rourkela-769 008, India.

May 14, 2015

Certificate

This is to certify that the work in the thesis entitled *Development of Local Feature Extraction and Reduction Schemes for Iris Biometrics* by *Beeren Sahu*, bearing roll number 612CS6003, is a record of an original research work carried out by him under our supervision and guidance in partial fulfillment of the requirements for the award of the degree of *Master of Technology (Research)* in *Computer Science and Engineering*. Neither this thesis nor any part of it has been submitted for any degree or academic award elsewhere.

Banshidhar Majhi
Professor

Pankaj K. Sa
Assistant Professor

Acknowledgment

I owe deep gratitude to the ones who have contributed greatly in completion of this thesis.

Foremost, I would like to express my sincere gratitude to my advisor, Dr. Pankaj K. Sa for providing me with a platform to work on challenging areas of biometrics. His profound insights and consistent notation in my writings have been true inspirations to my research.

I am grateful to my co-supervisor, Prof. Banshidhar Majhi who has provided me with continuous encouragement and support to carry out my research. His dedication and attention to details has motivated me to work for excellence.

I am very much indebted to Prof. Bidyut Kumar Patra and Prof. Ashok Kumar Turuk for providing insightful comments at different stages of thesis that were indeed thought provoking.

My special thanks go to Prof. Gopal Krishna Panda and Prof. Munshi Nurul Islam for contributing towards enhancing the quality of the work in shaping this thesis.

I would like to thank all my friends and lab-mates for their encouragement and understanding. Their help can never be penned down with words.

Most importantly, none of this would have been possible without the love and patience of my family. My family to whom this dissertation is dedicated to, has been a constant source of love, concern, support and strength all these years. I would like to express my heartfelt gratitude to them.

Beeren Sahu

Abstract

Iris is one of the most reliable biometric trait used for human recognition due to its stability and randomness. Typically, recognition concerns with the matching of the features extracted from the iris regions. A feature extraction method can be categorized as local or global, depending on the manner in which the features are extracted from an image. In case of global features fail to represent details of an image because, the computation is focused on the image as a whole. On the contrary, local features are more precise and capable of representing the details of an image as they are computed from specific regions of the image. In the conventional approaches, the local features consider corners as keypoints, that may not always be suitable for iris images.

Salient regions are visually pre-attentive distinct portions in an image and are appropriate candidate for interest points. The thesis presents a salient keypoint detector called Salient Point of Interest using Entropy (SPIE). Entropy from local segments are used as the significant measure of saliency. In order to compute the entropy value of such portions, an entropy map is generated. Scale invariance property of the detector is achieved by constructing the scale-space for the input image.

Generally local feature extraction methods suffer from high dimensionality. Thus, they are computationally expensive and unsuitable for real-time application. Some reduction techniques can be applied to decrease the feature size and increase the computational speed. In this thesis, feature reduction is achieved by decreasing the number of keypoints using density-based clustering. The proposed method reduces keypoints efficiently, by grouping all the closely placed keypoints into one. Each cluster is then represented by a keypoint with its scale and location, for which an algorithm is presented. The proposed schemes are validated through publicly available databases, which shows the superiority of the proposed ones over the existing state-of-the-art methods.

Keywords: *Iris biometrics, feature extraction, feature reduction, salient points, scale-space, clustering.*

Contents

List of Figures

List of Tables

List of Algorithms

List of Acronyms

ACC Accuracy

CBIR Content Based Image Retrieval

DBSCAN Density-Based Spatial Clustering of Applications with Noise

DoG Difference-of-Gaussian

EER Equal Error Rate

FAR False Acceptance Rate

FRR False Rejection Rate

GAR Genuine Acceptance Rate

LDA Linear Discriminant Analysis

LoG Laplacian-of-Gaussian

NNDR Nearest Neighbor Distance Ratio

PCA Principal Component Analysis

PILP Phase Intensive Local Pattern

PILPR Phase Intensive Local Pattern Reduced

ROC Receiver Operating Characteristic

SIFT Scale Invariant Feature Transform

SPIE Salient Points of Interest using Entropy

SPIER Salient Point of Interest using Entropy Reduced

SURF Speeded-Up Robust Feature

Chapter 1

Introduction

Biometrics is the science of recognizing the identity of an individual based on physiological and behavioral characteristics of the subject. Automated biometrics attempt to mimic a fundamental human attribute to distinguish and recognize other people as individual and unique. This automation is achieved through a combination of hardware and pattern recognition algorithms. Here, hardware implies to biometric scanner like, fingerprint scanner in the case of fingerprint biometrics or iris scanner in the case of iris biometrics. There is a long history of using distinguishing marks for identification. From hand-impressions on cave walls and hand-written signatures on documents to the measurement of unique patterns of Morse operators, there has been longing to use and measure biometric identity [1]. The usage of computers to identify people from their physical and behavioral attributes dates back to the digital computer evolution of the 1960s. However, even after decades of research and hundreds of projects the field of biometrics still remains fresh and challenging. Worldwide over the past few years, there has been a marked increase in both government and private sector interest in massive biometric deployments for accelerating humanmachine interaction, efficiently delivering human services, fighting identity fraud and even battling terrorism [2].

A generic biometric system operates by taking an input from an individual, preprocess the input to find the region of interest, extract features, and authenticate

the individual [3]. A biometric system usually has three operating modes: enrollment mode, verification mode, and identification mode. Figure 1.1 illustrates the three modes of biometric system. In enrollment mode, the feature from a subject is extracted and stored in the database. During verification mode, a subject is authenticated by comparing live query biometric template with the database template of the individual whom the subject claims himself to be. The comparison in this mode is a one-to-one process. In identification mode, the system takes live query template from the subject and searches the entire database to find the best-match template to identify the subject. The comparison in this mode is a one-to-many process.

Due to tremendous need of security in an automated system, various biometric traits like face, iris, fingerprint, gait, voice, face-thermograph, signature are key areas of research. Observing underlying nature of the traits, two basic categories can be identified as: Physiological (or passive) and Behavioral (or active) biometrics. Physiological biometrics are based on direct measurement or data derived from measurement of a part of the human body. A person is identified by his/her face by another person. Fingerprint detection is one of the age-old methods used for recognizing the authenticity of a person. However, iris pattern, retina tissue pattern, palmprint geometry have evolved as leading physiological biometrics with the evolve of automation of biometric recognition system. Behavioral characteristics are the actions taken by a person. Behavioral biometrics, in turn, are based on measurements of data derived from an action, and thereby indirectly measure characteristics of the human body. Voice recognition, keystroke dynamics, and online/offline signature are some leading behavioral biometric traits. To ensure a trait to be able to serve as biometric token, it must satisfy following criteria:

- **Distinctiveness or uniqueness:** A biometric should have features that allow high levels of discrimination in selecting any particular individual while rejecting everyone else. The larger the number of people to be distinguished, the more important this factor becomes.

- **Stability:** Age, and perhaps accident or disease, may change a trait over a period of time. A biometric should preserve enough features so that these changes will have a minimal effect on the system's ability to discriminate. Stability may be of less significance where re-enrollment can be simply or easily achieved, or where re-issue over shorter duration is legally required.

- **Scalability:** A biometric should be capable of being processed efficiently, both at acquisition time and when it is searched in a database for identification-based access. Scalability issues may be less of a concern for verification-based access control systems than for large identification systems.

- **Usability:** A major basis for the adoption of biometrics is its convenience. If a biometric is difficult or slow to use, it would probably not be adopted. There is also a question of acceptance of the trait by some social or religious sect.

- **Inclusiveness:** An extremely high proportion of the population should be measurable, particularly for large-scale identity systems.

- **Insensitivity:** Changes in the external environment (e.g., lighting, temperature) within reasonable boundaries should not cause system failures due to malfunction of the trait.

- **Vulnerability**: It should be difficult to create a fake prosthetic biometric (known as spoofing), or to steal and use a detached one.

- **Privacy:** Ideally the permission of the owner of a biometric should need to be sought before acquisition of the trait. A trait should not be easily captured without a person's notice or permission.

Iris is a unique trait which satisfies all the aforesaid criteria. In this thesis we have investigated on iris biometric system.

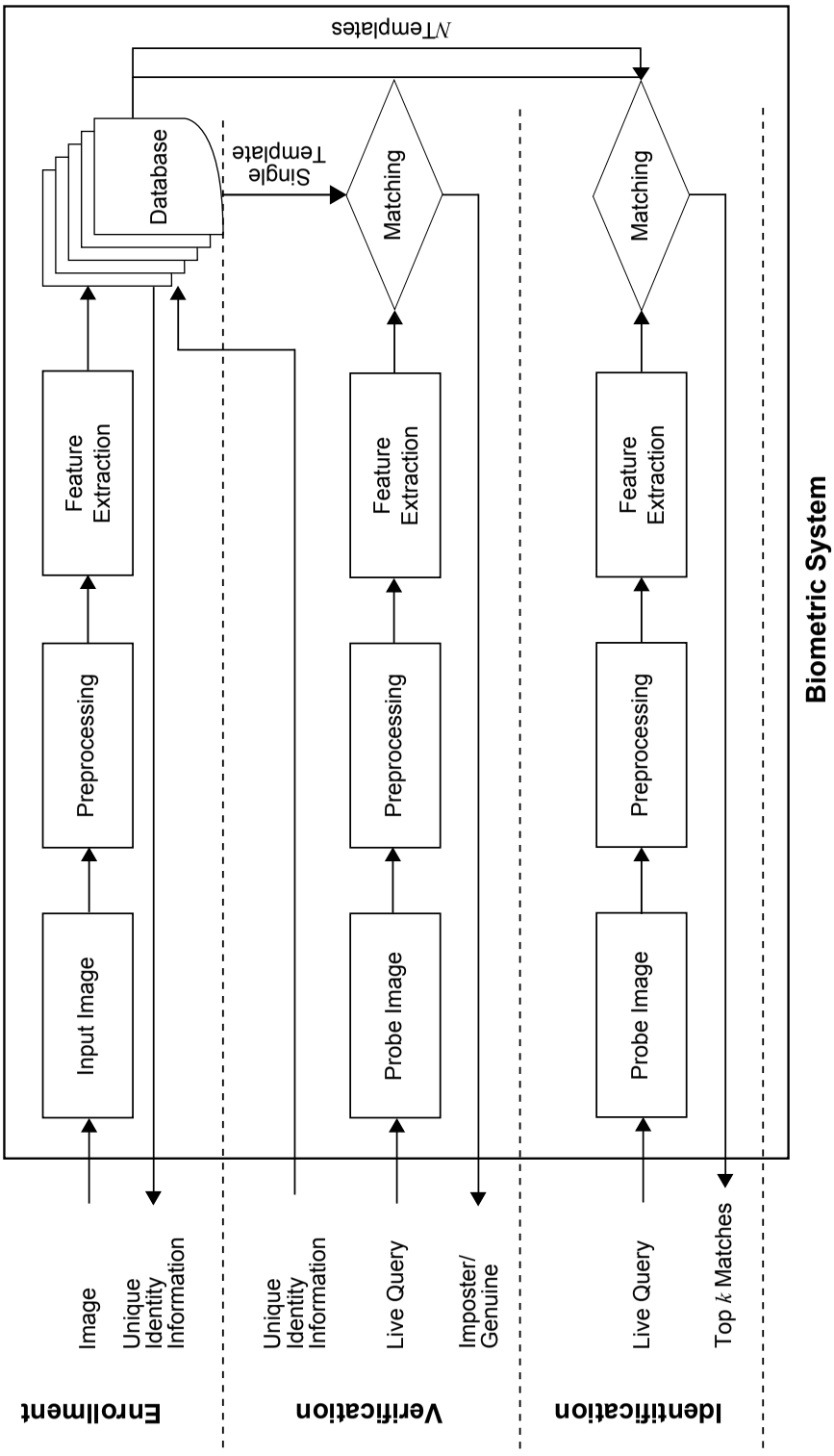

Figure 1.1: Modes of biometric authentication

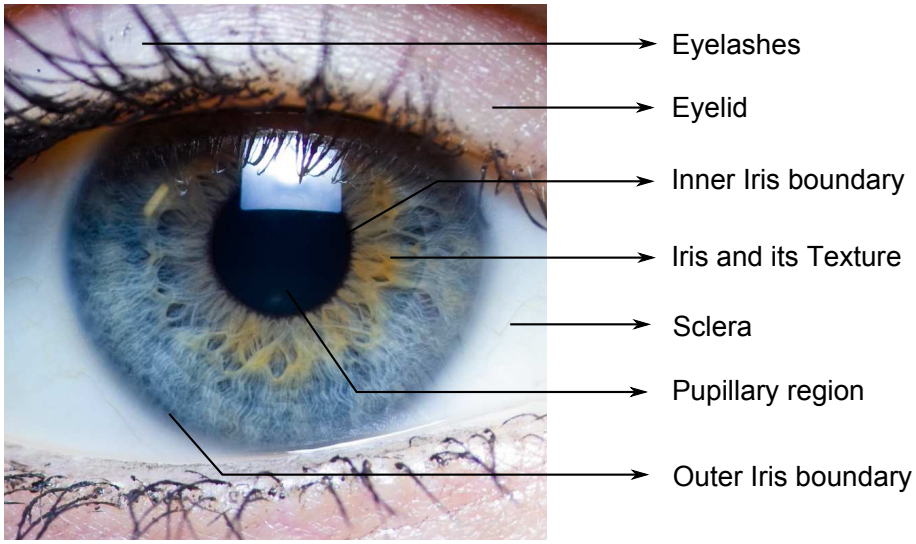

Figure 1.2: Anatomy of human eye

1.1 Iris Biometrics

The anatomy of human eye is depicted in Figure 1.2. Pupil is the darkest circular shaped area in the eye image. Pupil controls the amount of light entering the eye by dilation and contraction. Iris is an internal organ that is well protected against damage and scour by a highly transparent membrane (the cornea). This distinguishes it from fingerprint, which easily wears off with age and makes it difficult to recognize. Most significant features (viz. freckles, coronas, stripes, furrows, crypts) in the eye image are in the iris. It has a fine texture, determined randomly during embryonic gestation and is unique. Even genetically identical individuals have completely independent iris textures. Thus making it ideal for human recognition with high confidence. The randomness of the flowery pattern in iris is unique for every individual and hence can work as a token for authenticating an individual. An unimplemented conceptual design of an iris biometric system is first proposed by Leonard Flom and Aran Safir [4]. The first prototype unit for biometric system was developed in 1995 by L. Flom, A. Safir, and J. Daugman. Further, research establishes iris to be a candidate for reliable and non-cooperative biometric authentication. Iris, due to its stability and ease of acquiring, plays a

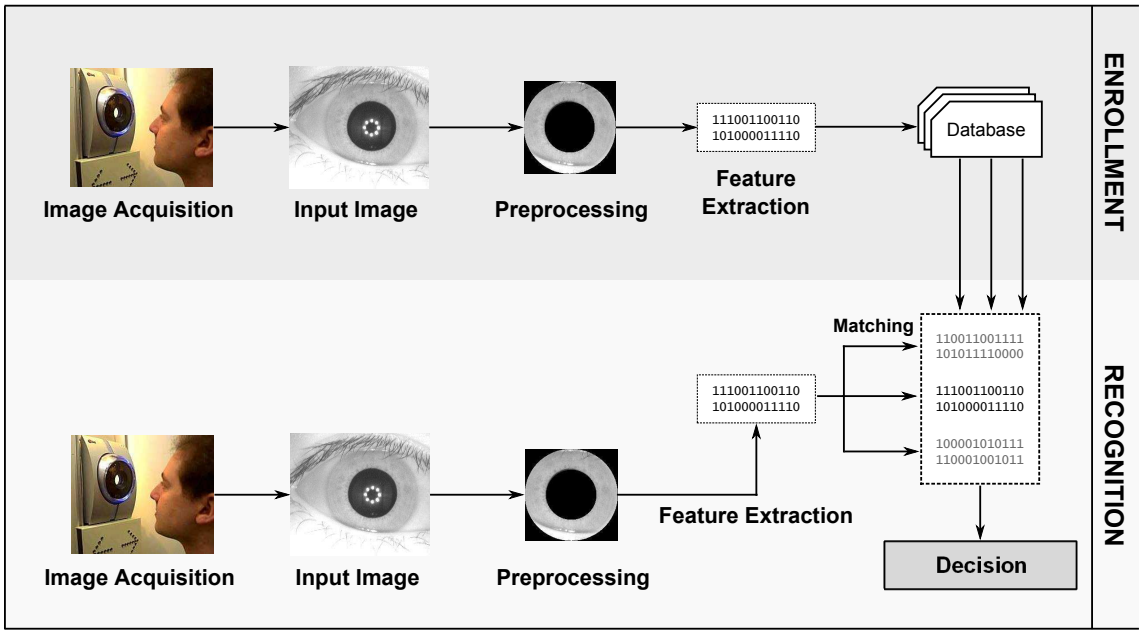

Figure 1.3: Block diagram of iris biometric system

significant role among all the biometric traits. The general block diagram of iris biometric system is shown in Figure 1.3.

Recent authentication systems need secure, fast, and accurate computing for which iris pattern is found to be suitable. Furthermore iris image can be captured without active cooperation of the subject. This marks the suitability of iris recognition also for criminal identification. Iris biometric system involves challenges of automating the system to identify the region of interest, finding useful feature(s) from the region of interest, matching two features when a query comes, maintaining feature sets corresponding to every enrolled subject in the database etc. All these segments are independent research areas and forms an authentication system when deployed together.

1.2 Motivation

Analyzing the texture of the iris has been the most popular area of research in iris biometrics [5]. The global feature extraction approaches fail to work under change

in rotation, scaling, illumination, and viewpoint of two iris images. In last few decades, good amount of works have been done for recognition; however, iris based identification is still in its infancy and needs careful attention. Efficient extraction and reduction of the local features are the challenges within the field of computer vision, especially for real-time applications. The main objectives of any feature extraction technique are, high efficiency and less computation time.

Scale Invariant Feature Transform (SIFT) [6] and Speeded-Up Robust Feature (SURF) [7] are most popular local feature extraction techniques known till date. They are widely used in Object Recognition and Content Based Image Retrieval (CBIR), because of their robustness and repeatability. Even though they are used in iris recognition [8–12], they suffer from two of the major shortcomings. Firstly, they consider corners in an image as keypoints. Secondly, their descriptors do not take texture information into account. An iris image predominantly has random patterns. It is rich in texture and does not have prominent corners unlike objects. Hence corners cannot be considered as keypoints in iris images, and they can be best described through texture analysis.

A keypoint denotes to a point of "interest" in an image. Edges and corners can be considered as interest point and region around them as a feature. Edge points and corners are the locations within the image where rapid changes in intensity take place. In other words, these are the points where there is high randomness. It is very well known that entropy is a measure of randomness. So, all points within an image having entropy greater than some threshold are interest points. Thus making them a suitable candidate for keypoints. Another reason for applying the entropy-measure for detection is that, it is used to measure the strength of detected keypoints [13]. A feature point descriptor with greater entropy value implies more information content in the descriptor, thus making it more discriminant. And it is very well known that, a more discriminative descriptors lead to better recognition.

One of the major advantages of local feature is its superior accuracy, but at the same time it suffers from high dimensionality. Such high dimensional features are

time consuming, thus making them unsuitable for real-time applications. Hence, in addition to feature extraction, reduction techniques can be applied to further decrease the size of the feature and increase the speed of the authentication system. However, reduction of feature may lead to fall in accuracy. Therefore, the system has to tradeoff between time and accuracy, depending on the system requirements. There are two approaches of reducing the feature size: (a) dimensionality reduction and (b) keypoint reduction. In this thesis, we have suggested a feature reduction scheme for dense descriptors like Phase Intensive Local Pattern (PILP) [14], where the second approach is an obvious choice. Here, groups of closely placed keyoints are clustered and each represented by single keypoint.

1.3 Iris Databases

This section discusses in detail about the databases used in all experiments relevant to the research in this thesis. The proposed system has been tested on two publicly available databases, viz. BATH and CASIAv3. Database available from BATH University [15] includes images from 50 subjects. For each subject, 20 images from each eye are captured. Database from Chinese Academy of Sciences' Institute of Automation contains eyes acquired in an indoor environment. CASIA version 3 (CASIAv3) [16] is a superset of CASIAv1. In version 3, most of the images have been captured in two sessions with an interval of at least one month. CASIAv3 database comprises 16213 iris images from 819 eyes. Figure 1.4 presents sample images from each iris database.

1.4 Performance Measures

The match score generated after testing with user given template and database template is deterministic (0:imposter, and 1:genuine) in case of knowledge based or token based authentication system. It is a process of matching two alphanumeric

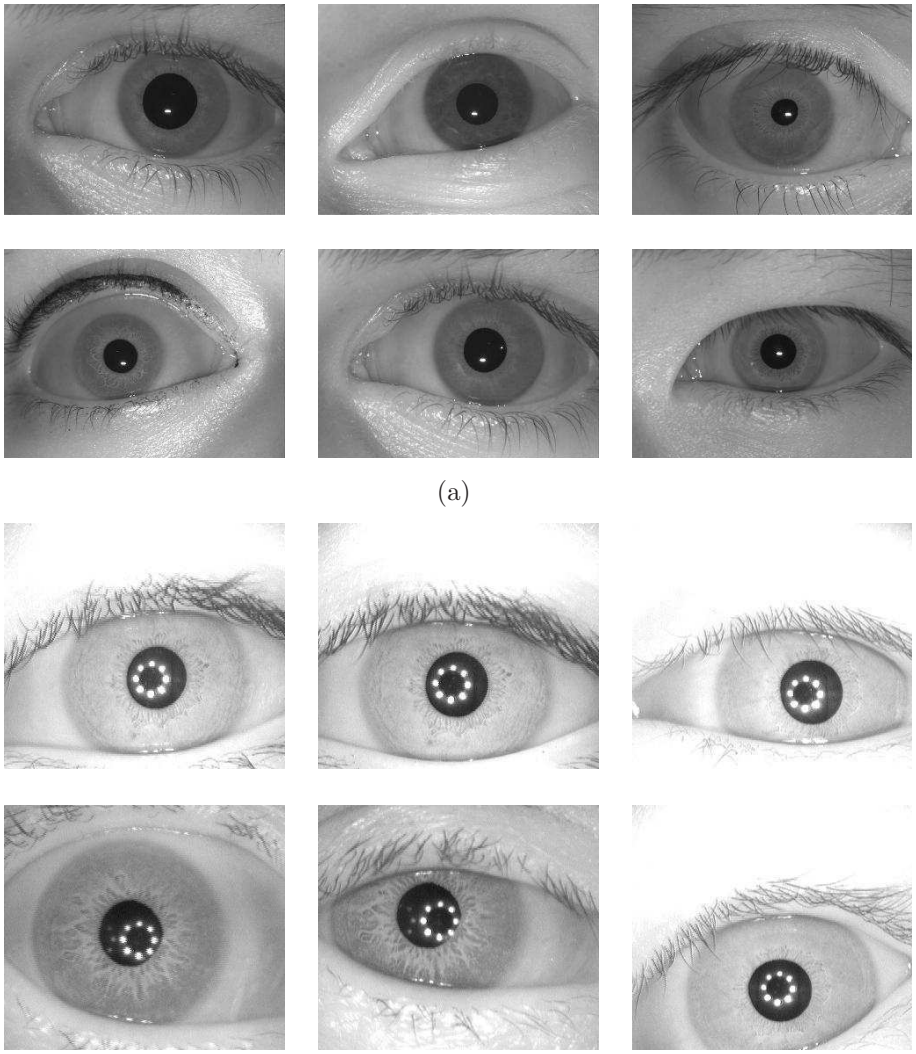

(a)

(b)

Figure 1.4: Sample iris images from: (a) BATH and (b) CASIAv3 databases

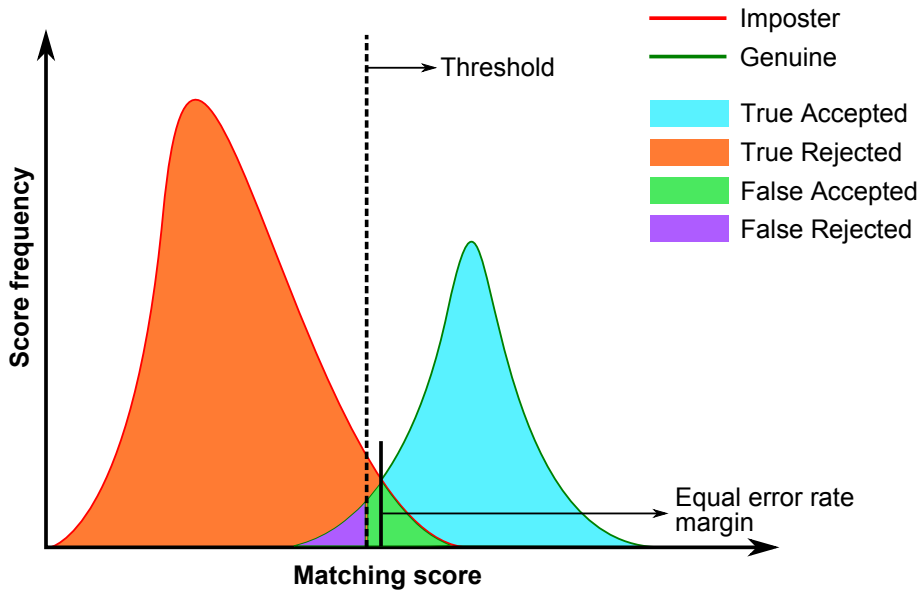

Figure 1.5: Genuine and imposter matching score distribution of biometric database showing various performance measures

strings (e.g. password submitted by the subject and corresponding password stored in database). However the matching of biometric templates are more complex due to the reason that n-dimensional biometric templates have no sorted ordering. The second challenge in this domain is that the templates of query and database image do not match exactly due to noise. Hence the matching problem is more of pattern matching. The matching module in the biometric system is responsible for generating a score when a query template and a database template are given as input to it. The generated score is a numerical value signifying extent to which the query template resembles the database template. Hence the system needs a threshold to decide the genuinity of the query template. Any score above the decided threshold is concluded as an genuine match. Likewise any score below the threshold is concluded as a imposter match. If the threshold is chosen very high, the system would lead some genuine matches to be judged as imposter, which is otherwise known as False Rejection. On the contrary, if the threshold is chosen very low, the system would lead some imposter matches to be judged as genuine or False Acceptance. The choice of threshold value is therefore bears profound significance.

Similarity scores or genuine-scores are generated when two biometric templates of the same subject are compared. This type of score is called genuine-score or intra-class variation. The set of feature chosen should be such that intra-class variation is small. Likewise when two biometric templates of two different subjects are compared, inter-class variation score (imposter-score) is generated. The values of imposter-scores should be high enough to be discriminating from the genuine-scores. However, the distribution of genuine-scores and imposter-scores are not mutually exclusive in practical scenarios; rather, they are overlapped. While recognition, the scores that exceed a chosen threshold value (τ), results in false acceptance. The genuine score that falls below τ results in false rejection. Figure 1.5 shows the representation of few performance measures. The commonly used measures to evaluate the performance of biometric systems are:

- **False Acceptance Rate (FAR):** FAR is the frequency of fraudulent access to imposters claiming identity [17]. This statistic is used to measure biometric performance when operating in the verification mode. A false accept occurs when the query template of an individual is incorrectly matched to existing biometric template of another individual.

- **False Rejection Rate (FRR):** FRR is the frequency of rejections relative to people who should be correctly verified. This statistics is used to measure biometric performance when operating in the verification mode. A false reject occurs when an individual is not matched correctly to his/her own existing biometric template.

- **Equal Error Rate (EER):** ERR is the point where FAR is equal to FRR. In general, the lower the equal error rate value, the higher the accuracy of the biometric system. Note, however, that most operational systems are not set to operate at the equal error rate, so the measure's true usefulness is limited to comparing biometric system performance. EER is sometimes referred to as the *Crossover Error Rate*.

- **Genuine Acceptance Rate (GAR):** GAR is the fraction of genuine scores exceeding the threshold τ. It is defined as:

$$GAR = 1 - FRR \tag{1.1}$$

- **Receiver Operating Characteristic (ROC) Curve:** ROC curve depicts the dependence of FAR with GAR for change in the value of threshold. The curve is plotted using linear, logarithmic or semi-logarithmic scales. ROC can also be represented by plotting FRR against FAR for change in the threshold value.

1.5 Contribution in the Thesis

In this thesis there are two major contributions as follows:

Feature Extraction: Salient Points of Interest using Entropy (SPIE):

A keypoint detection scheme using entropy is proposed specifically for textured images like iris. SPIE detects salient keypoints from the textured region in iris of an individual for efficient feature extraction. Salient regions are visually pre-attentive distinct portions in an image. Entropy from local segments within an image is used as the significant measure of saliency. To know the entropy value of such portions, an entropy map is generated. Salient keypoint detection is performed using SPIE, and subsequently each point is represented using Speeded-Up Robust Feature (SURF) descriptor. The similarity score is obtained using nearest neighbor distance ratio. This is further discussed in detail in the **Chapter 2** of the thesis.

Feature Reduction Scheme using Density-based Clustering:

A scheme is suggested to reduce the number of keypoints detected by a keypoint detector. Density-based clustering is applied to group the keypoints together; those are placed very close to each other. Each cluster of keypoints can be then

represented by a single keypoint. Each cluster along with the noise points forms the new set of keypoints. SURF is then used to describe these keypoints and the similarity score is obtained using nearest neighbor distance ratio. Details of the above are presented in the **Chapter 3** of the thesis.

The last chapter of the thesis depicts the analytical remarks to overall achievements and limitations of all the proposed works, concluding with scope for further research work in this domain.

Chapter 2

Feature Extraction: Salient Points of Interest using Entropy (SPIE)

The very beginning and most substantial step in pattern recognition is feature extraction. It is required to transform the image to some reduced feature space for the efficient exercise of any image processing operation. A feature extraction method can be categorized as local or global, depending on the manner in which the features are extracted from an image. One of the most widely used global feature in iris recognition is Gabor filter based feature, proposed by John Daugman [18]. There are many notable work in global feature [18–38] extraction for iris recognition. However, global features fail to represent details of an image as they are computed over the image as a whole. On the contrary, local features are more precise and capable of representing the details of an image as they are computed from specific regions of the image. Such regions can be identified around some unique points in the image, known as *interest points* or *keypoints* and the feature extracted from these regions are known as *keypoint descriptor*. Thus, in any local feature extraction technique, keypoint detection and keypoint description are the two important steps. Figure 2.1 shows the general steps involved in the process of local feature extraction for iris image.

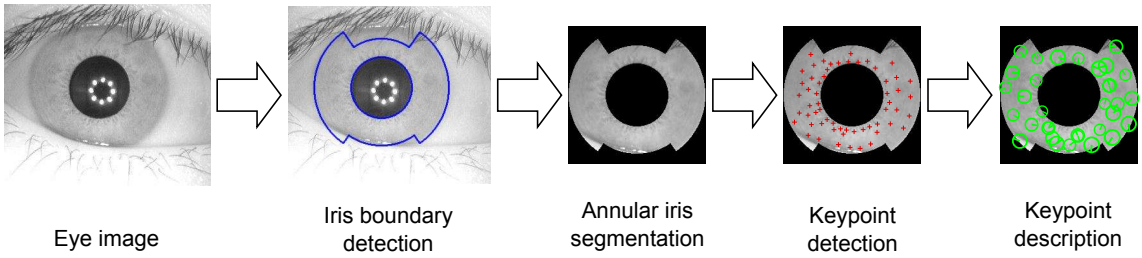

Figure 2.1: Local feature extraction for iris image

Scale Invariant Feature Transform (SIFT) [39] and Speeded-Up Robust Feature (SURF) [7] are the two most popular local feature extraction technique known till date. They are widely used in *object recognition* and *Content Based Image Retrieval* (CBIR), because of their robustness and repeatability. Even though they are used in iris recognition [10, 11], they suffer from a few major shortcomings; such as, they consider only corners as keypoints and their descriptors do not take texture information into account. So an efficient local feature extraction technique is required, to make use of the random patterns present in iris. Alternatively, some salient regions in the image can be considered as keypoints.

The suggested iris recognition scheme adopts local feature extraction technique, so as to explore the rich texture information in the iris. A keypoint detection method is introduced and various popular feature descriptors are used to find suitable feature space to explicitly describe the iris texture. The objective of the proposed detector is to unearth the salient points in the iris texture. Conventional salient point detectors, compute keypoints solely at the given resolution and thus overlook the scale parameter. By representing the image at multiple scales, a detector can achieve scale invariance. Even though the proposed method embraces the multi-scale theory; however, defers in the manner of its usage.

This chapter is organized as follows. Few notable related work in keypoint detection are presented in Section 2.1. Proposed salient keypoint detection method is described in Section 2.2 and feature matching is discussed in Section 2.3. In Section 2.4, the experimental results are provided. Finally, the summary is presented at the end of this chapter.

2.1 Related Work

Early developments within the field of local keypoint detectors can be found in the work of Moravec [40]. His method tries to detect visible objects by reverting regions with high local directional variance. A local window is slightly sifted in various directions in the image and results in the average change of image intensities. This value gives the directional variance, and the method of computing these values is popularly known as Moravec operator. In the year 1988, Harris and Stephens developed Harris detector [41]. They noted that Moravec's corner detector can be closely related to the local auto-correlation function. This function identifies the edge and corner regions in an image. Moreover, it helps in determining the response of an edge or corner by taking trace and determinant into consideration. This detector is rotation-invariant; yet it is not scale-invariant. Harris-Laplace detector [42] developed during early 1990s, applies Harris's detector in a multi-scale image to achieve scale invariance. The modified auto-correlation matrix is adaptable to scaling changes, to make it invariant to variation in image resolution. The inconvenience of identifying a requisite and stable scale for features such as blobs, corners, edges, and ridges remained a challenge. Lindeberg [43] investigated same as a problem of scale selection. In the year 1994, he came up with the method of automatic scale selection, which was accomplished by finding local extrema over the scale-space. He also suggests the Gaussian function is the only scale-space kernel. Later in 2004, David Lowe proposed Scale Invariant Feature Transform (SIFT) detector, which is invariant to image translation, scaling, and rotation. Like Lindeberg, he also used Gaussian kernel in the construction of scale-space. Approximation of Laplacian-of-Gaussian (LoG) to Difference-of-Gaussian (DoG) [39] is the groundbreaking work by Lowe. The keypoints at maxima of the scale-space, applied with DoG function are selected. As a result, the preferred keypoints hold a high level of efficiency and achieve rotation invariance [44]. A comprehensive list of some of the popular keypoints detector is given below.

1981: Moravecs operator [40]

- Directional variance
- Used for object detection

1988: Harris corner detector [41]

- Auto-correlation function - eigen values
- Rotation invariant

1993: Harris-Laplacian detector [42]

- Harris points + Laplacian at different scales
- Scale invariant

1997: Smallest Univalue Segment Assimilating Nucleus (SUSAN) [45]

- Based on self dissimilarity
- Some resemblance with DoG features

1998: Laplacian of Gaussian (LoG) [43]

- Multi-scale representation
- Automatic scale selection

1999: Scale Invariant Feature Transform (SIFT) [6]

- Approximated LoG
- Invariant

2003: Scale & Affine Invariant Interest Point Detectors [46]

- Multi-scale representation Harris detector
- Invariant to scale and affine

2004: Affine Invariant Salient Region Detector [47]

- Entropy as saliency measure
- Repeatability under intra-class variability

2006: Features from Accelerated Segment Test (FAST) [48]

- Machine learning based corner detector
- It outperforms previous detectors

2008: Speeded-Up Robust Feature (SURF) [7]

- Fast Hassian matrix approximation
- Robust and fast

2008: Center Surround Extremas (CenSurE) [49]

- Simplified center-surround filters to approximate the Laplacian
- Claims to be better scale-space detectors

2009: Speeded Up Surround Extrema (SUSurE) [50]

- Modified CenSurE
- Accelerated the process by skipping the computation of the filter response

2010: Adaptive and Generic Accelerated Segment Test (AGAST) [51]

- Generates optimal decision tree for FAST using adaptive and generic segment test
- Improved FAST

2011: Binary Robust Invariant Scalable Keypoints (BRISK) [52]

- Multi-scale AGAST
- Lower computational cost

2.2 Salient Keypoint Detection

The primary step in any local feature extraction scheme requires identification of keypoints. A keypoint can be defined as a point of *interest* in an image. Edges and corners can be contemplated as interest point and region around them as a feature. These are the points in the image where rapid changes in intensities are recorded. In other words, these are the points where there is high randomness. It is very well known that entropy is a measure of randomness. So, all points within an image having higher entropy value are candidates to be interest points. Thus entropy is a suitable measure for the detection of keypoints. Moreover, a feature descriptor with larger entropy value generally implies higher information content and thus more

discriminatory. And it is very well known that more discriminative descriptors lead to better recognition.

Entropy has been used to detect salient regions in an image [47, 53, 54]. The term saliency is extensively used in *cognitive psychology* and *computer vision*. A salient region in an image refers to pre-attentively distinct region. In terms of image processing, *salient region* is a region that "stand-out" with respect to its neighborhood. Hence, a *salient point* in an image is literally almost unique point. Extensive studies on visual saliency for object recognition can be found in many recent works [47, 54–56]. Few noteworthy points are stated below.

- Salient points are local in nature.
- Local information alone are sufficient to describe the image contents.
- Performance of local descriptors using saliency for object recognition is comparatively better.
- Use of entropy measures to identify regions of saliency in an image [47, 53, 54].
- Salient points have higher entropy value [53].

2.2.1 Salient Point Detection using Entropy Map

Following are the major stages of computation used to detect salient points in an image:

- **Construction of Scale-Space:** For the given input image, the scale-space is constructed by convolving the image with variable-scale Gaussian filter as shown in Figure 2.2. The scale invariance property of a keypoint detector can be achieved with automatic scale selection in the Gaussian scale-space. The scale-space for the input image is constructed by smoothening it successively with Gaussian [43,57]. It is defined as a function $L(x, y, \sigma)$, which is generated

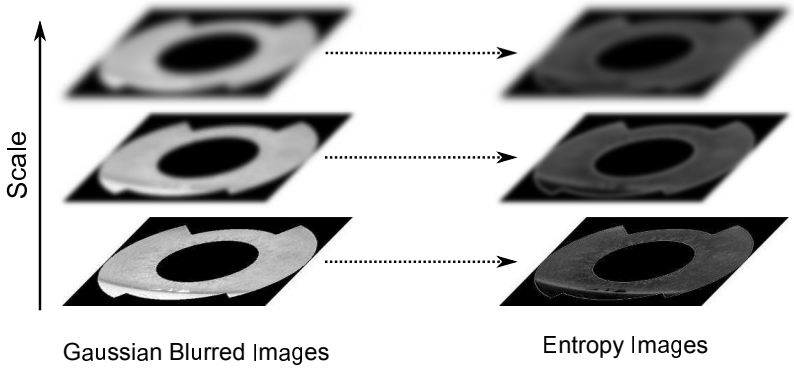

Figure 2.2: Scale-space construction and the corresponding entropy images

by convolving a variable-scale Gaussian filter $G(x, y, \sigma)$, with the input image $I(x, y)$:

$$L(x, y, \sigma) = G(x, y, \sigma) * I\,(x, y) \tag{2.1}$$

where $*$ is the convolution operation in x and y, and

$$G(x, y, \sigma) = \frac{1}{2\pi\sigma^2} e^{-\left(x^2+y^2\right)/2\sigma^2} \tag{2.2}$$

- **Computation of Entropy Map:** Keypoint can be considered as a point where there is high randomness; or in other words, high value of entropy. In order to identify such points, the entropy value is a prerequisite for each point. However, the challenge is in computing entropy for a point. To tackle this, an alternate representation of an image, known as *entropy map*, is introduced in this chapter. For each point in an image, entropy is computed for a small region around it. As a result, each point in the entropy map gives the entropy value for the corresponding point in the original image. Such entropy maps are computed for each blurred image in the scale-space.

  Considering different probabilities between states, entropy gives a general uncertainty measure [58]. This measure is popularly known as *Shannon's entropy*. For the given events occurring with probability P_i, the Shannon's

entropy is described as

$$H = \sum_{i=1}^{m} P_i \log \frac{1}{P_i} = -\sum_{i=1}^{m} P_i \log P_i \tag{2.3}$$

Similarly, Shannon's entropy can be evaluated for an image by considering the probabilities of the gray level distributions in the image. Hence the entropy of a gray image can be computed using,

$$\mathcal{H}(\mathbb{R}) = -\sum_{k=0}^{255} \mathcal{P}_k(\mathbb{R}) \log_2 \mathcal{P}_k(\mathbb{R}) \tag{2.4}$$

Here $\mathcal{H}(\mathbb{R})$ indicates entropy for the region $\mathbb{R}$ in gray image, and $\mathcal{P}_k$ means probabilities of the frequency of histogram in the region $\mathbb{R}$. Entropy map $\mathcal{E}(x, y, \sigma)$ is computed for the given blurred image $G(x, y, \sigma)$ in the scale-space, where the value of each point (x, y) in $\mathcal{E}(x, y, \sigma)$ is the entropy value computed for a window around corresponding pixel (x, y) in $G(x, y, \sigma)$. This map can be viewed as an image, termed as *entropy image*. Figure 2.4 shows the Difference-of-Gaussian (DoG) and entropy image for *Lena* and *Cameraman* images. Entropy image is shown in *gray* and *jet color-map* available in MATLAB, for better visual realization. While computing entropy map, it is important to determine the appropriate window size, such that the entropy value computed has certain significance. The window size depends upon the value of σ of the Gaussian filter with which the blurred image is generated [7]. For each blurred image in the scale-space, respective entropy map $\mathcal{E}(x, y, \sigma)$ is generated using the Algorithm 2.1 and an example is depicted in Figure 2.3.

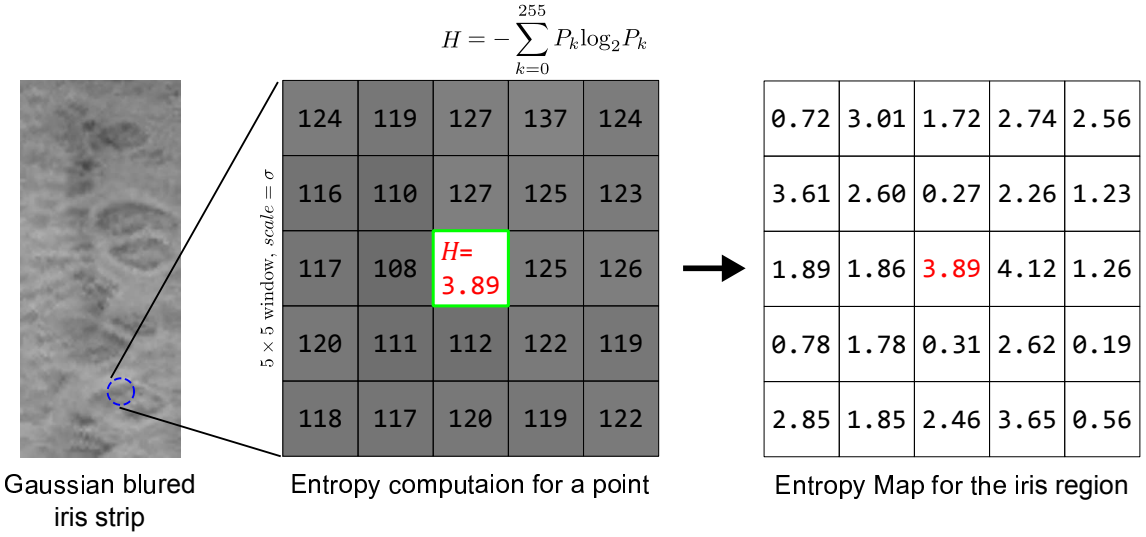

Figure 2.3: Computation of entropy map for a region in iris strip

Algorithm 2.1 Generate_Entropy_Map

Input: G: Gaussian Blurred Image, σ: Sigma value of the Gaussian kernel.
Output: $\mathcal{E}_{map}$: Entropy Map

1: **for** each point (i, j) in G **do**
2: $\quad \mathbb{R} \leftarrow wSize \times wSize$ sized window
3: $\quad \mathcal{E}_{map}(i, j, \mathbb{R}) \leftarrow -\sum_{k=0}^{255} \mathcal{P}_k(\mathbb{R}) \log_2 \mathcal{P}_k(\mathbb{R})$
4: **end for**
5: **return** $\mathcal{E}_{map}$

- **Keypoint Localization:** Finally, local maxima are detected in the scale-space. Each candidate point is compared with its 3×3 neighborhood in same scale, the scales above, and below, as shown in Figure 2.5. A point is selected only if its value is larger in comparison to all of its neighbors. Subsequently, if the selected point is greater than some threshold, then it is accepted as a stable keypoint.

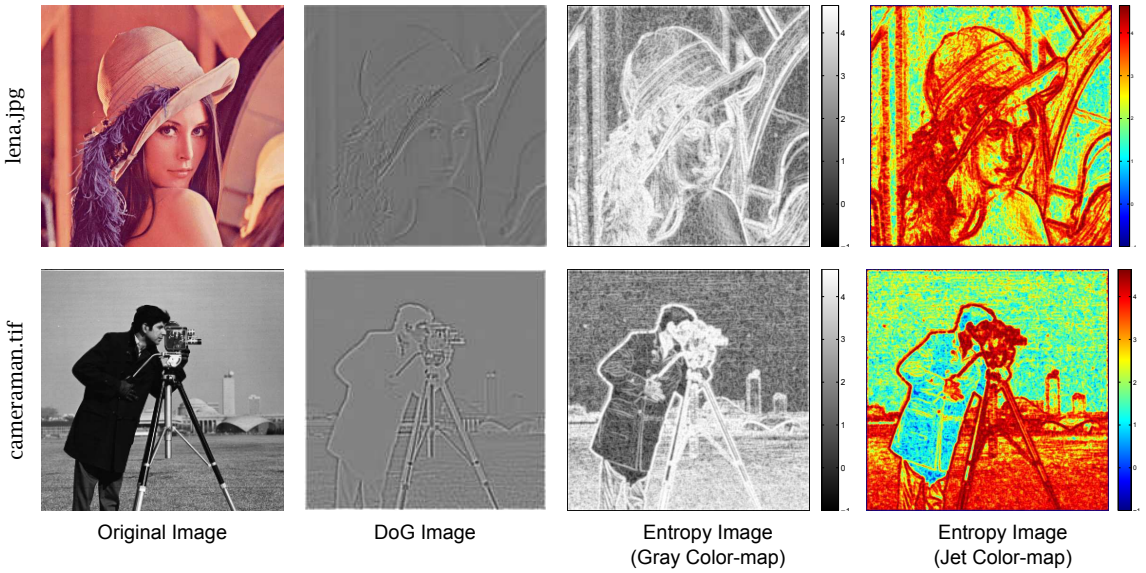

Figure 2.4: Difference-of-Gaussian (DoG) and entropy image for *Lena* and *Cameraman* image

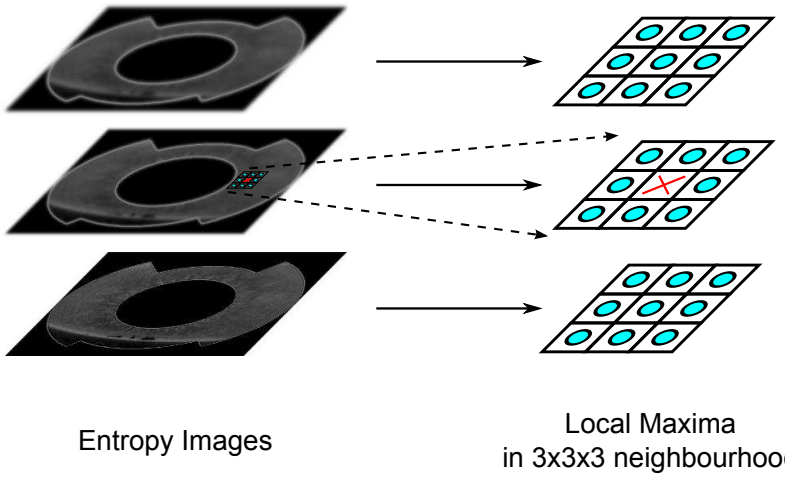

Figure 2.5: Maxima detection from the entropy image in the scale-space

2.3 Matching

After keypoints are detected, they are described using a fast and robust local descriptor, Speeded-Up Robust Feature (SURF) [7]. SURF features are matched using nearest neighbor distance ratio (NNDR) for Euclidean distance between them, given by:

$$NNDR = \frac{d_1(u,v)}{d_2(u,v)} \tag{2.5}$$

Where, $d(u,v)$ is the Euclidean distance defined as,

$$d(u,v) = \left(\sum_i (u_i - v_i)^2 \right)^{1/2} \tag{2.6}$$

In (2.5), d_1, d_2 are the two nearest distances while matching. Smaller is the ratio, better will be the match.

2.4 Experimental Evaluation

To evaluate the performance of the proposed keypoint detection technique, SURF descriptor is used and compared with few popular feature extraction techniques. All methods are tested on publicly available BATH and CASIAv3 databases. Local features are extracted from the segmented annular iris images [9]. Figure 2.6 demonstrates the SPIE keypoints with their scales and orientations. Accuracies for various methods are calculated from the ROC curve and are given in Table 2.1. It may be observed that the proposed SPIE has a higher accuracy for both the databases. Figure 2.7 depicts the ROC curve for each method. The distribution of genuine and impostor similarity scores for the proposed method is shown in the Figure 2.8. Here, the similarity score is the NNDR ratio computed for any genuine or impostor pair of irises.

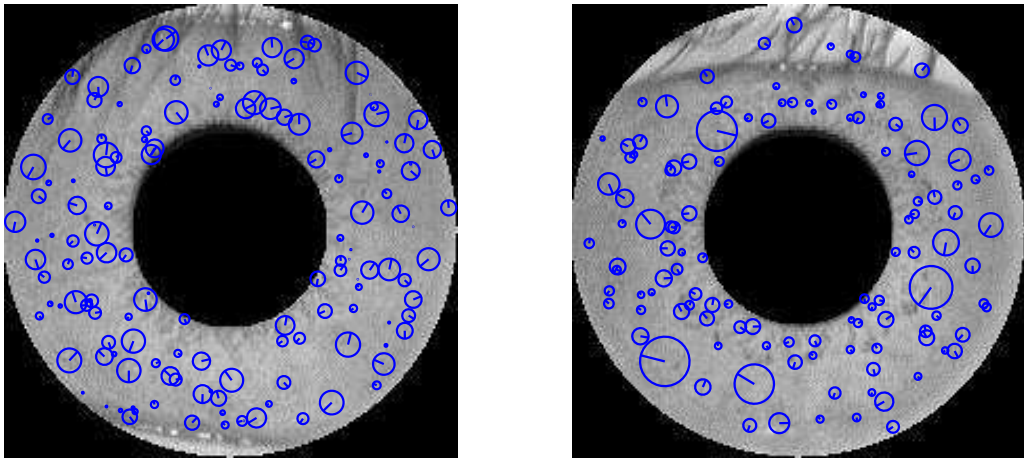

Figure 2.6: Keypoints with scale and orientation using proposed SPIE (sample iris images from CASIAv3)

Table 2.1: Performance measures for SIFT, SURF and proposed method

Databases →	**BATH**			**CASIAv3**		
Approaches ↓	**ACC**	**FAR**	**FRR**	**ACC**	**FAR**	**FRR**
SIFT	89.82	6.29	17.32	92.59	4.03	11.63
SURF	92.39	4.35	10.32	94.72	4.69	6.73
Proposed SPIE	94.23	3.48	7.69	96.33	2.85	5.23

2.5 Summary

In this chapter, a salient keypoint detection method, SPIE is proposed, particularly for textured iris images. It is compared with two state-of-the-art local features [6, 7], and the accuracy is found to be 94.23% for BATH and 96.33% for CASIAv3. For both the databases the accuracy obtained is more in comparison to other two methods with least false acceptance and rejection rate. This escalation in result is because the proposed method is capable of unearthing salient keypoints present in the textured iris image.

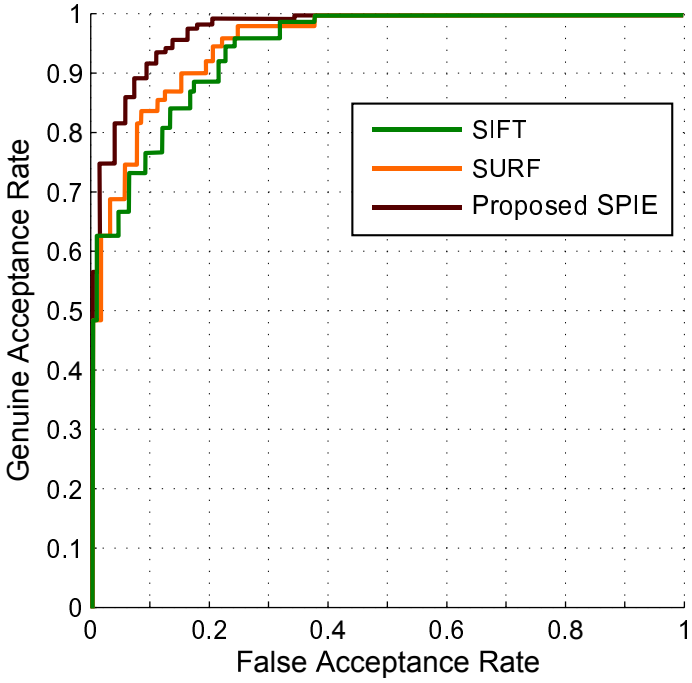

(a) BATH Database

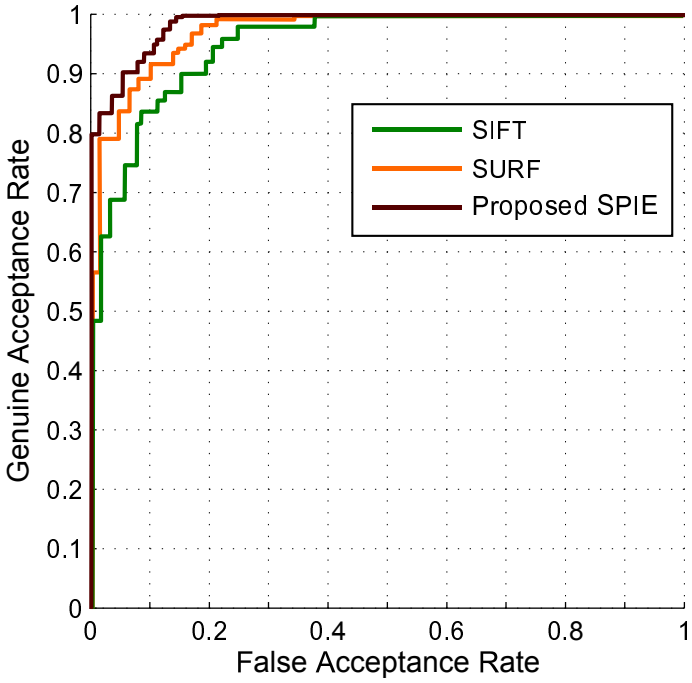

(b) CASIAv3 Database

Figure 2.7: ROC curve for SIFT, SURF and proposed SPIE

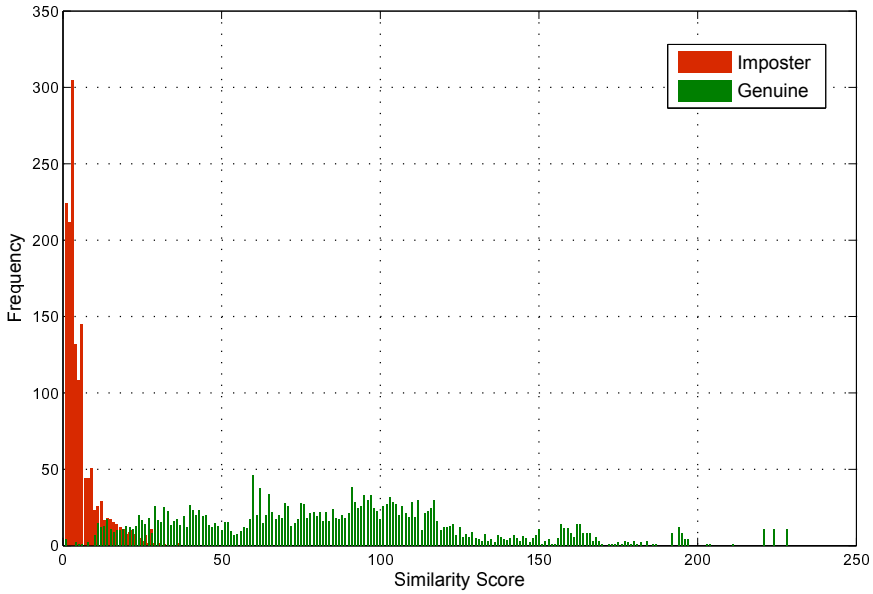

(a) BATH Database

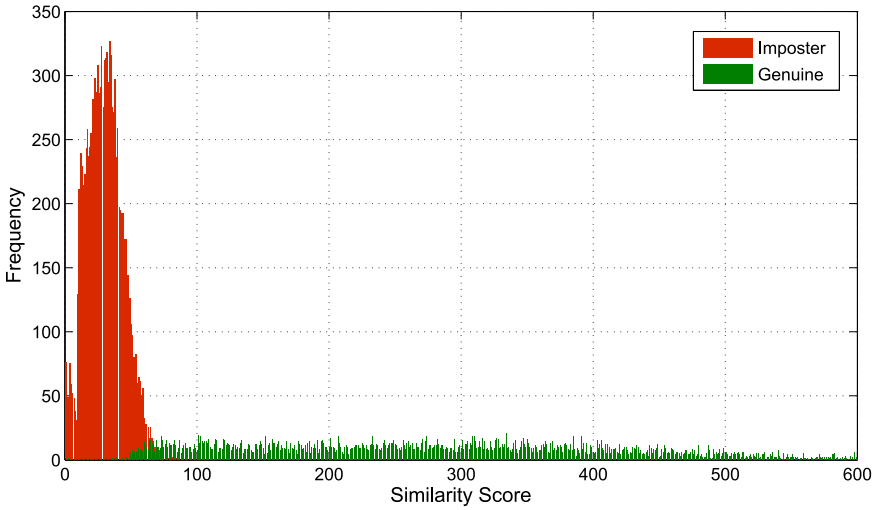

(b) CASIAv3 Database

Figure 2.8: Score distribution for SPIE

Chapter 3

Feature Reduction Scheme using Density-based Clustering

Local features are generally parameterized in very high dimensional spaces. This confines the execution of feature matching systems in terms of speed. Reduction can be achieved, either by compressing the dimension of feature vector or by reducing the number of detected keypoints. The proposed method reduces keypoints efficiently, by grouping all the closely placed keypoints into one. The overall feature reduction and extraction scheme is depicted in Figure 3.1. Each steps are discussed in details in the following subsections.

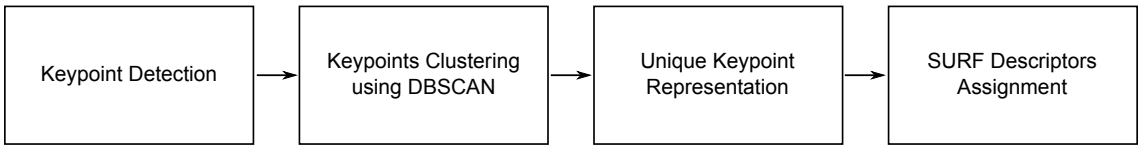

Figure 3.1: Block diagram for keypoint reduction of local features

This chapter is organized as follows. Few notable related works in feature reduction are presented in Section 3.1. Suggested reduction scheme for SPIE is described in Section 3.2 and in Section 3.3, reduction scheme for PILP is discussed. Finally, the summary is presented at the end of this chapter.

3.1 Related Work

One of the early work in the direction of reduction of local features is PCA-SIFT [59]. It is proposed by Ke *et al.* for the dimensionality reduction of SIFT descriptor. It projects the high dimensional feature vector of SIFT onto a lower dimension using Principal Component Analysis (PCA). It reduces the descriptor and also able to reduce the presence of high frequency noise in it. Hua and his fellow researchers at Microsoft Research Lab, observed PCA-SIFT to be less discriminative [60]. They suggested a similar reduction technique using Fisher analysis (LDA), that separate data well in the feature sub-space.

In a different approach to the priors, Alitappeh *et al.* reduced SIFT descriptor by applying Subtractive Clustering [61]. They decreased the size of features by removing keypoints those possessed high degrees of similarity with others. These remaining keypoints were more distinctive than the omitted ones. In another work Rudinac *et al.* reduced the number of keypoints of local features in two stages [62]. In first stage; they rejected points close in a specified neighborhood using a spatial criterion followed by selecting strong keypoints with high entropy. Yuasa *et al.* proposed a measure for robustness and distinctiveness of the local feature based on diverse density [63]. Based on this measure, they identified keypoints as strong or weak. Stronger keypoints lead to better matching.

In this chapter, we attempt to reduce the keypoints generated by SPIE and PILP [14] and compared their performances.

3.2 Feature Reduction for Salient Points of Interest using Entropy (SPIE)

Initially, keypoints are extracted using SPIE detector and their location and scale information are recorded. Subsequently, a clustering technique is utilized to reduce the number of keypoints. Among all clustering algorithm, density-based is best

suited as it do not assume cluster to have a fixed number of cluster nor any particular shape. Another reason for using density-based clustering is that it allows noise points that do not belong to any of the cluster. Such noise points are isolated keypoints that are discriminative and do not need to be part of any cluster.

3.2.1 Clustering of keypoints using DBSCAN

Cluster can be defined as a task of grouping similar points (data) together. Typically, within a cluster the density of points is considerably high in comparison to its neighbor. Density-based spatial clustering of applications with noise (DBSCAN) identify clusters by checking the ϵ-neighborhood of each object in the dataset. Any such object within the ϵ-neighborhood is said to be density-reachable. It then iteratively collects directly density-reachable objects from these core objects, which may involve the merging of a new density-reachable cluster. The process terminates when no new object can be added to any cluster.

Following are few important definitions related to DBSCAN [64]:

Definition 3.2.1 (ϵ-neighborhood) *Let D be a database, then ϵ-neighborhood of a point p, denoted by $N_\epsilon(p)$, is defined by*

$$N_\epsilon(p) = \{q \in D | dist(p, q) \leq \epsilon\}$$

Definition 3.2.2 (direct density-reachable) *A point p is directly density-reachable from a point q if*

$$1. p \in N_\epsilon(q)$$
$$2. |N_\epsilon(q)| \geq minPts$$

Figure 3.2 illustrates the core and border points, and direct density-reachable points in a cluster.

Definition 3.2.3 (density-reachable) *A point p is density-reachable from a point*

q, if there is a chain of points $p_1, \ldots, p_n$*, where,* $p_1 = q$ *and* $p_n = p$ *such that* p_{i+1} *is directly density-reachable from* p_i*.*

Definition 3.2.4 (density-connected) *A point p is density-connected to a point q, if there is a point o such that both, p and q are density-reachable from o.*

Figure 3.3 depicts the concept of density-reachability and density-connectivity.

Definition 3.2.5 (cluster) *Let D be a database of points. A cluster C is an non-empty subset of D satisfying the following conditions:*

1. $\forall p, q \in C$ *and q is density-reachable from p, then* $q \in C$*.*

2. $\forall p, q \in C$*: p is density-connected to q.*

Definition 3.2.6 (noise) *Let* $C_1, \ldots, C_k$ *be the clusters of database D, a noise is defined as the set of points in D not belonging to any cluster,*

$$noise = \{p \in D | \forall i : p \notin C_i\}$$

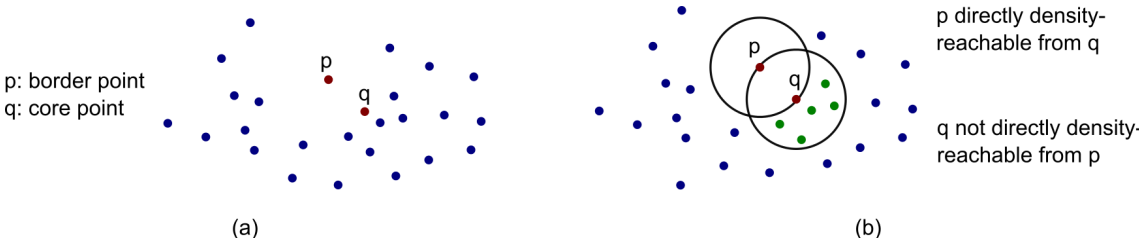

Figure 3.2: DBSCAN: (a) core and border points (b) direct density-reachability

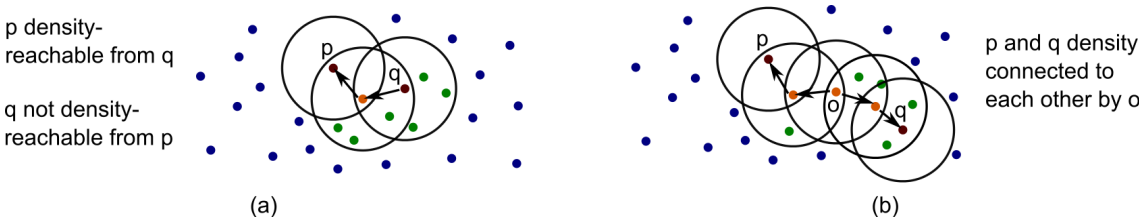

Figure 3.3: DBSCAN: (a) density-reachability (b) density-connectivity

Algorithm 3.1 DBSCAN

Input: D, eps, $minPts$
Output: C and $Noise$: set of cluster and noise points respectively

```
1: initialize C ← 0 and Noise ← 0
2: while P ∈ D and P.visited ≠ TRUE do
3:    P.visited ← TRUE
4:    NeighborPts ← epsNeighborhood(P, eps)
5:    if sizeof(NeighborPts) < minPts then
6:       Noise ← Noise ∪ P
7:    else
8:       expandCluster(P, NeighborPts, C, eps, minPts)
9:    end if
10: end while
11: return [C, Noise]
```

Algorithm 3.2 expandCluster

Input: $P, NeighborPts, C, eps, minPts$
Output: C

```
1: C ← C ∪ P
2: for each point P' in NeighborPts do
3:    if P'.visited == FALSE then
4:       P'.visited ← TRUE
5:       NeighborPts' ← epsNeighborhood(P', eps)
6:       if sizeof(NeighborPts') >= minPts then
7:          NeighborPts ← NeighborPts ∪ NeighborPts'
8:       end if
9:    end if
10:   if P' ∉ C then
11:      C ← C ∪ P'
12:   end if
13: end for
```

Algorithm 3.1 and 3.2 states the algorithm for DBSCAN. Here, an arbitrary point is selected among the points that have not been visited before and is marked *visited*. Its ϵ-neighborhood is retrieved using $epsNeighborhood$ method. If it contains sufficiently many points, then a cluster formation begins. Otherwise, this point is considered to be a noise. Now all point within the $epsNeighborhood$ added to the selected point as its own $epsNeighborhood$ if they are dense enough. This procedure

proceeds until the density-connected cluster is totally found. Subsequently, the algorithm starts over again for a new unvisited point.

We have used DBSCAN to bundle up closely placed keypoints those basically are parts of an individual larger feature. Thus intuitively, they can be represented by a unique keypoint and there by assisting in reducing the number of keypoints naturally and efficiently. Figure 3.4 illustrates the formation of clusters from keypoints detected using DBSCAN in a iris patch.

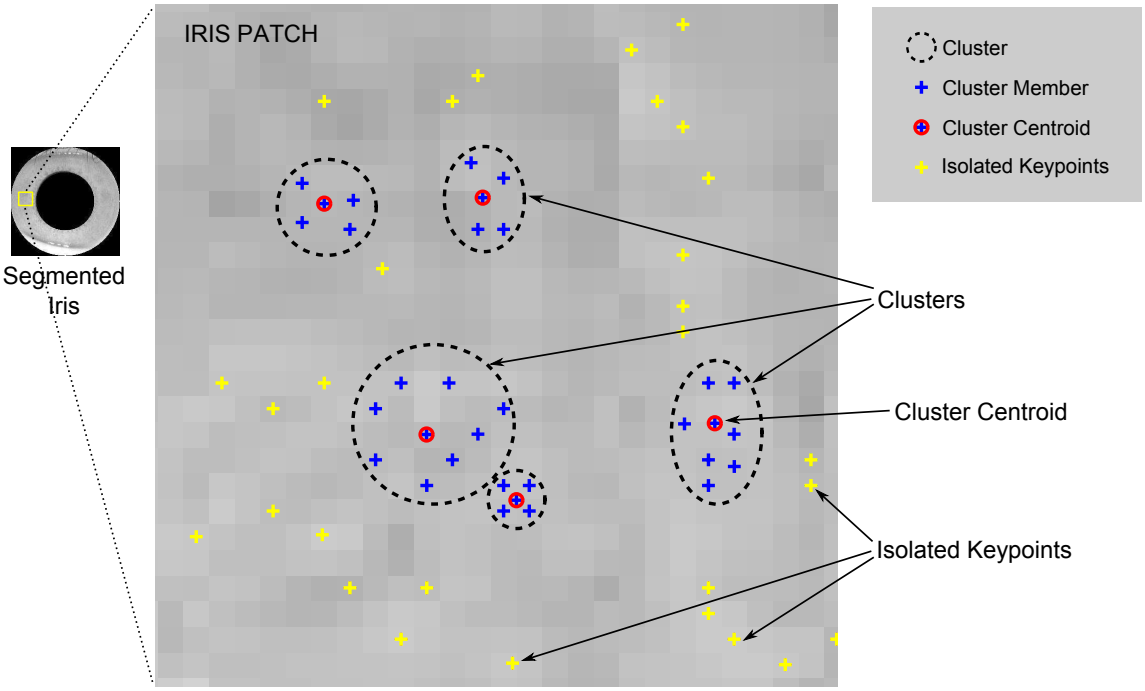

Figure 3.4: Cluster formation from keypoints in a iris patch

3.2.2 Unique keypoint representation

Each cluster obtained from DBSCAN along with noise points, forms the new set of reduced keypoints. Noise points are actually the isolated keypoints and are included directly to the new set of keypoints. However, each cluster requires to be represented by a new keypoint. Any keypoint, requires its location and scale information to describe it using a local descriptor. The geometric centroid of the cluster is assigned

as the new location for the keypoint. Whereas, the scale can be determined using the scale-space theory [43, 57, 65]. The scale-space is constructed by convolving an image with variable scale Gaussian kernels. For each scale, there is a specific size of the Gaussian filter [7]. In other words, if the size of the window is known, then the scale can be determined as they are related. Based on this hypothesis, we determine the scale from the diameter of the cluster using the Algorithm 3.3 and depicted in Figure 3.5. Here, the diameter of the cluster is identical to the window size of the feature formed by the cluster in the scale-space.

Definition 3.2.7 (Window size) *The window size of a keypoint is the size of the mask taken around a keypoint to represent its scale at which the feature has been detected.*

Definition 3.2.8 (Cluster diameter) *The diameter of the cluster is the twice of the sum of the maximum possible distance between the centroid to any keypoint within the cluster and half of the window size of that keypoint.*

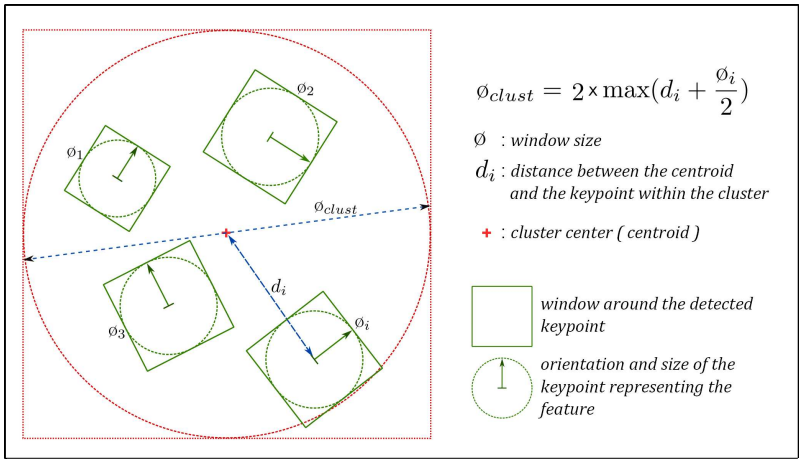

Figure 3.5: Determination of scale (window size) for a cluster of keypoints.

Algorithm 3.3 Cluster_keypoint_representation

Input: $C := \{C_1, C_2, \ldots, C_n\}$: Clusters of keypoints
$where, C_i := \{kp_1, kp_2, \ldots, kp_m\}$
Output: $KP[Scale, LOC] := \{KP_1, KP_2, \ldots, KP_n\}$: new set of keypoints

1: **for** each cluster C_i in C **do**
2: $cent_i := centroid(C_i)$
3: $d_{max} := \underset{j}{max}[distance(cent_i, kp_j)]$
4: $\phi_i := 2 \times \left[d_{\max} + \frac{\phi_{kp_j}}{2}\right]$
5: $LOC_i := cent_i$
6: $Scale_i := \alpha.\phi_i$
7: $KP_i := [Scale_i, LOC_i]$
8: **end for**
9: **return** KP

3.2.3 Experimental Evaluation

To evaluate the performance, all methods are tested on publicly available BATH and CASIAv3 databases. Accuracy for various methods are calculated from the ROC curve and are mentioned in the Table 3.1. Performance of the reduced SPIE has been found inferior compared to the state-of-the-art detectors: SIFT [6] and SURF [7]. Empirically, it is validated that keypoints produced by SPIE are optimal. Hence, there is no scope for further reductions. Figure 3.6 depicts the ROC curve for each method. The distribution of genuine and impostor scores for the proposed reduction scheme for SPIE is shown in the Figure 3.7. The time comparison for various methods are shown in the Table 3.2. The proposed reduction method (SPIER) is also compared with a similar reduction scheme using k-means clustering (SPIER(k-means)). Here, k value is set to three-quarters of the total number of keypoints. Figure 3.8 shows the effect of k on accuracy of the reduction scheme.

Table 3.1: Performance of various local features

Databases →	**BATH**			**CASIAv3**		
Approaches ↓	**ACC**	**FAR**	**FRR**	**ACC**	**FAR**	**FRR**
SIFT	89.82	6.29	17.32	92.59	4.03	11.63
SURF	92.39	4.35	10.32	94.72	4.69	6.73
SPIE	94.23	3.48	7.69	96.33	2.85	5.23
SPIER	85.33	5.72	11.55	87.39	5.33	7.15
SPIER (k-means)	69.36	10.94	19.70	73.54	8.71	17.75

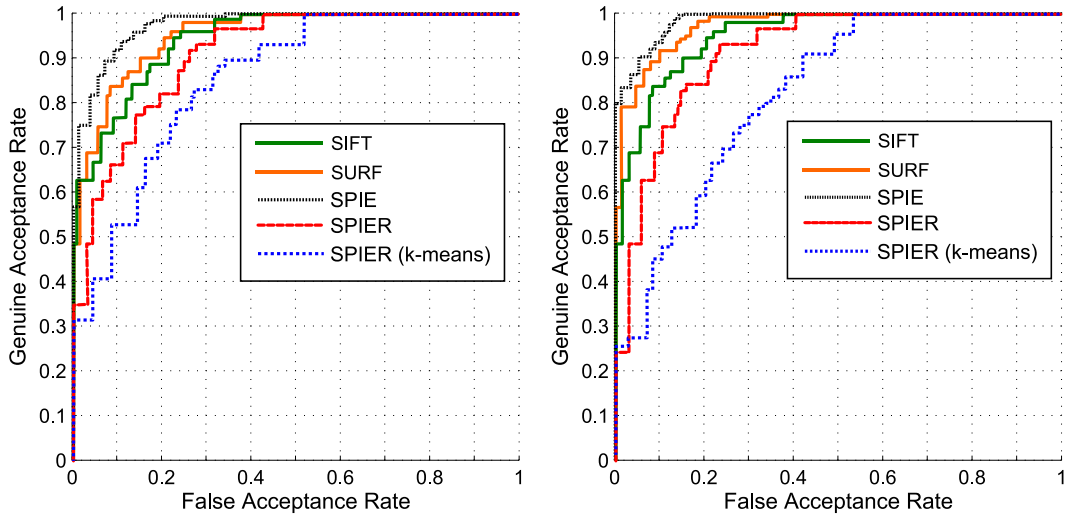

(a) BATH Database (b) CASIAv3 Database

Figure 3.6: ROC curve for various local features

Table 3.2: Time (in seconds) comparison for various local features

Databases →	**BATH**			**CASIAv3**		
Approaches ↓	**Average #keypoints**	**Average time (extraction)**	**Average time (matching)**	**Average #keypoints**	**Average time (extraction)**	**Average time (matching)**
SIFT	131.47	0.38	3.94	364.07	1.13	10.92
SURF	13.60	0.16	0.40	62.03	0.36	1.86
SPIE	10.23	1.53	0.36	54.74	4.93	1.64
SPIER	5.69	1.58	0.29	19.17	4.97	1.03
SPIER (k-means)	7.53	1.55	0.26	42.35	4.95	1.26

3.3 Feature Reduction for Phase Intensive Local Pattern (PILP)

To validate the suggested feature reduction scheme, we tried it on an existing feature known as Phase Intensive Local Pattern (PILP). It is capable of extracting high dimensional subtle local features existing in iris region. It detects a sufficiently large number of densely packed keypoints, giving an excellent recognition accuracy. However, it is computationally very expensive. The large number of detected keypoints causes the extraction and recognition process considerably slow.

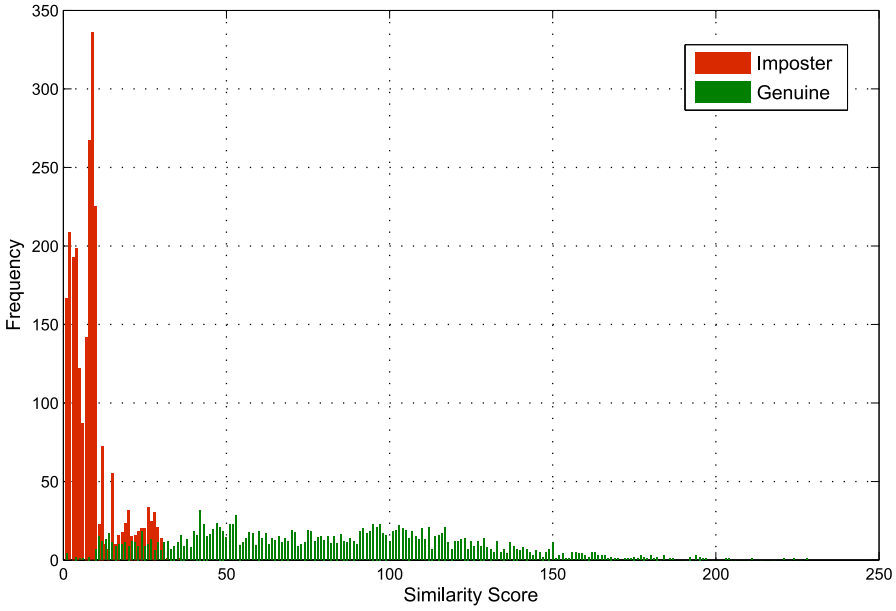

(a) BATH Database

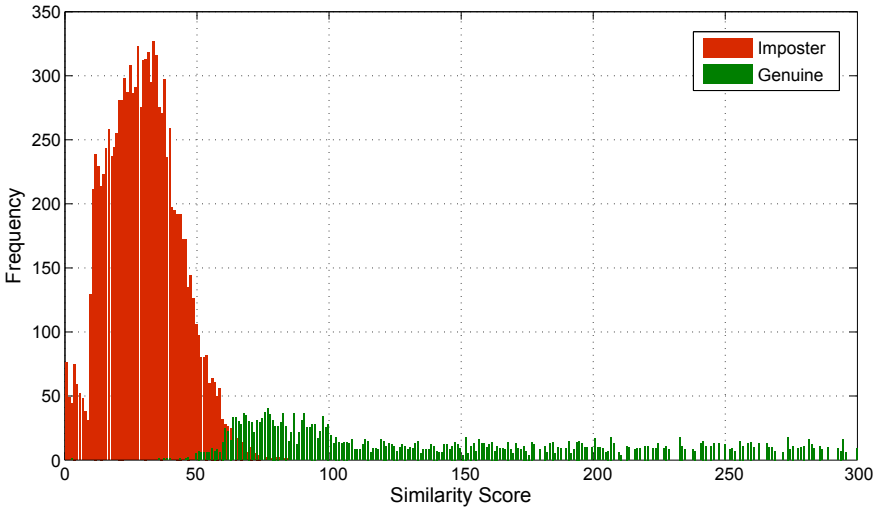

(b) CASIAv3 Database

Figure 3.7: Score distribution for reduced SPIE

3.3.1 Keypoints Detection using PILP

Keypoint detection through Phase Intensive Local Pattern (PILP) [14] is obtained with a variable size filter depending on different scales. These scales are varied from 3 to 9 at a step of 2. Correspondingly the filters' size also increases from 3×3 to

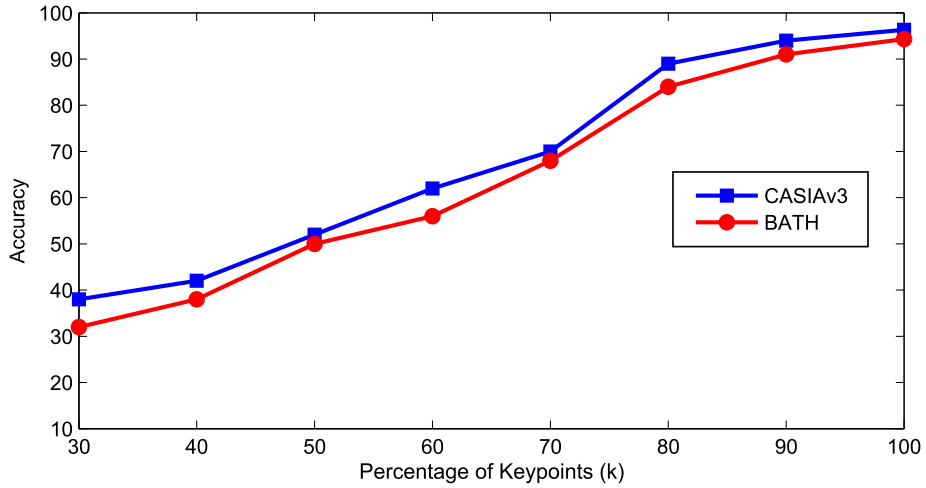

Figure 3.8: Effect of k on accuracy

9×9. At a given scale Δ, the PIP at a pixel (x_c, y_c) with respect to its $\Delta^2 - 1$ neighbors considering a phase-tilt ϕ can be derived using (3.1). For each scale, the value of ϕ is varied from 0 to $\frac{7\pi}{4}$ with an leap of $\frac{\pi}{4}$, resulting eight filters as shown in Figure 3.9. It is found that only four out of these filters are unique, as shown in Figure 3.10. Finally for each pixel location in the convolved image for each scale, local extrema are identified as potential keypoints. Now selecting a suitable threshold value, high enough to eliminate the edge features. Figure 3.11 illustrates the whole PILP keypoint detection method and summarized in Algorithm 3.4.

$$
\begin{aligned}
PILP(x_c, y_c, \Delta, \phi) &= \frac{\sum_{n=1}^{\Delta^2-1} s(i_n, i_c).2^{\sin\left(\tan^{-1}\left(\frac{y_n - y_c}{x_n - x_c}\right) - \phi\right)}}{\sum_{n=1}^{\Delta^2-1} 2^{\sin\left(\tan^{-1}\left(\frac{y_n - y_c}{x_n - x_c}\right) - \phi\right)}} \\
&= \sum_{n=1}^{\Delta^2-1} \left(s(i_n - i_c). \left(\frac{2^{\sin\left(\tan^{-1}\left(\frac{y_n - y_c}{x_n - x_c}\right) - \phi\right)}}{\sum_{n=1}^{\Delta^2-1} 2^{\sin\left(\tan^{-1}\left(\frac{y_n - y_c}{x_n - x_c}\right) - \phi\right)}} \right) \right)
\end{aligned}
\tag{3.1}
$$

where, $s(i_n, i_c) = 1$ if $i_n \geq i_c$ and $s(i_n, i_c) = 0$ if $i_n < i_c$

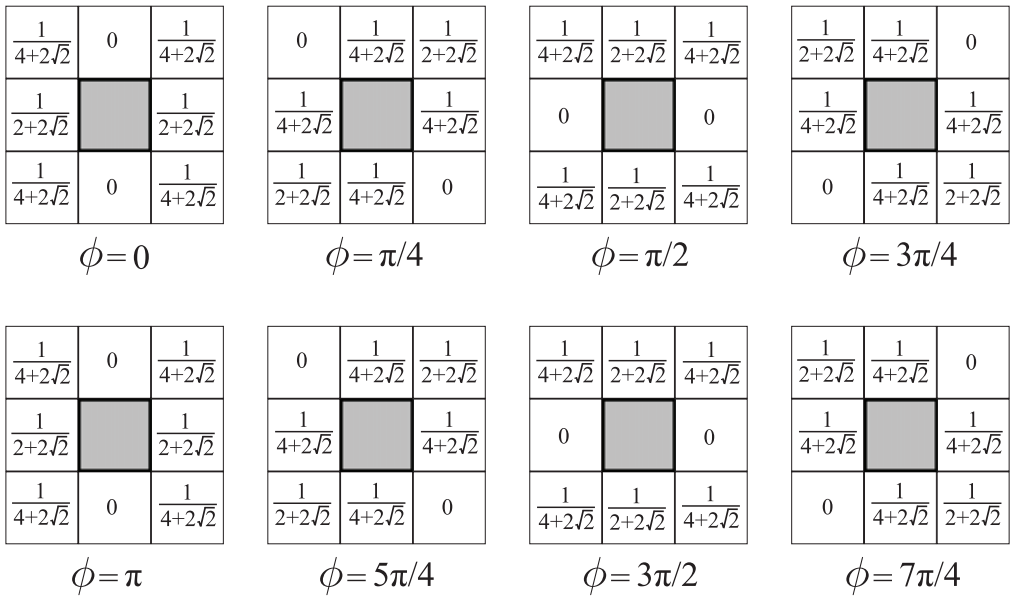

Figure 3.9: PILP filter bank [14]

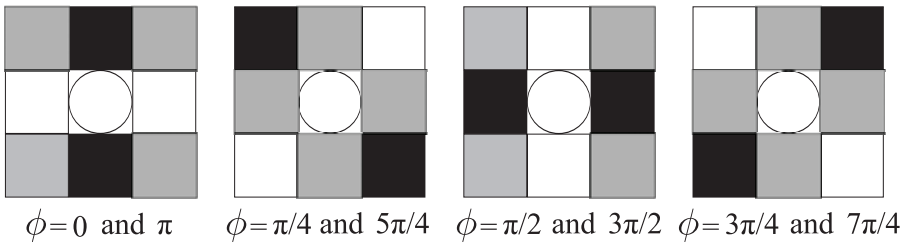

Figure 3.10: Intensity representation of the PILP filter bank [14]

3.3.2 Feature Reduction using Density-based Clustering

Keypoints detected from PILP are reduced using the proposed reduction scheme previously discussed in Section 3.2.

3.3.3 Feature Descriptor

Authors of the PILP feature applied SIFT descriptor to represent their keypoints, which suffers from high dimensionality and longer execution time. Speeded-up

Algorithm 3.4 Keypoint_Extraction_PILP

Input: I: Original image; F_3, F_5, F_7, F_9: Filter banks
Output: K: Extracted keypoints from I

for $\Delta := 3$ to 9 **do**
  $K_\Delta \equiv \Phi$
  for $i := 0$ to $3\pi/4$ **do**
    $I_{\Delta,i\pi/4} \leftarrow I \oplus f_{\Delta,i\pi/4} \oplus s$
    $i \leftarrow i + \pi/4$
  end for
  for $i := 0$ to $3\pi/4$ **do**
    for each pixel (x, y) in $I_{\Delta,[i \mod 4]\pi/4}$ **do**
      if $I_{\Delta,[i \mod 4]\pi/4}(x, y)$ is extrema among its neighbours in $I_{\Delta,[i \mod 4]\pi/4}$, $I_{\Delta,[(i-1) \mod 4]\pi/4}$, and $I_{\Delta,[(i+1) \mod 4]\pi/4}$ **then**
        $K_\Delta \leftarrow K_\Delta \cup (x, y)$
        $i \leftarrow i + \pi/4$
      end if
    end for
  end for
  $\Delta \leftarrow \Delta + 2$
end for
$K \leftarrow K_3 \cup K_5 \cup K_7 \cup K_9$
return K

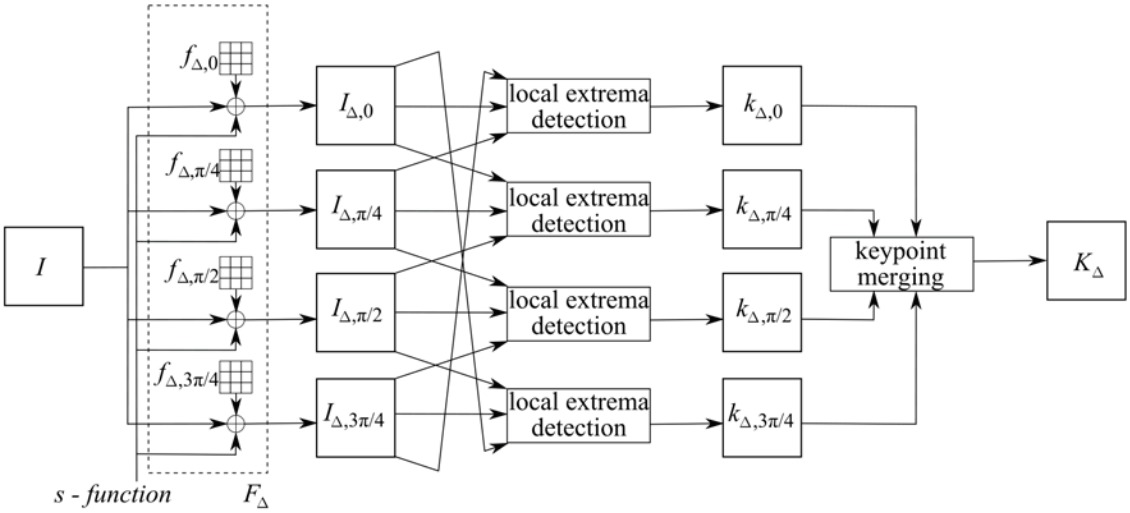

Figure 3.11: PILP keypoint extraction method [14]

Robust Feature (SURF) [7] is much faster and low dimensional feature compared to Scale Invariant Feature Transform(SIFT) [39], and with almost same accuracy due to its distinctiveness and repeatability. SURF uses only 64 dimensions compared to SIFT using 128 dimensional vector. This reduces feature computation time and allows quick matching with increased robustness simultaneously. A circular window is constructed around every detected keypoint and orientation is estimated using Haar Wavelet responses to have invariance to rotation. Further, SURF descriptors are obtained by taking a rectangular window around every detected keypoint in the direction of orientation. The windows are split into 44 sub regions and Haar wavelet responses extracted in horizontal and vertical direction are summed up. The wavelet responses are summed up along with the absolute values to find the polarity of image intensity changes. Thus summing up the descriptor vectors from all 44 sub-regions, feature descriptor of length 64 is obtained. The descriptor vector of length 64 for each interest point forms feature vector.

3.3.4 Experimental Evaluation

To evaluate the performance, all methods are tested on publicly available BATH and CASIAv3 databases. To assess the performance of the proposed extraction and reduction techniques, accuracy for various methods are calculated from the ROC curve and are mentioned in the Table 3.3. Figure 3.12 depicts the ROC curve for each method. The distribution of genuine and impostor scores for the proposed reduction scheme for PILP is shown in the Figure 3.13. The time comparison for various methods are shown in the Table 3.4. The proposed reduction method (PILPR) is also compared with a similar reduction scheme using k-means clustering (PILPR(k-means)). Here, k value is set to three-quarters of the total number of keypoints.

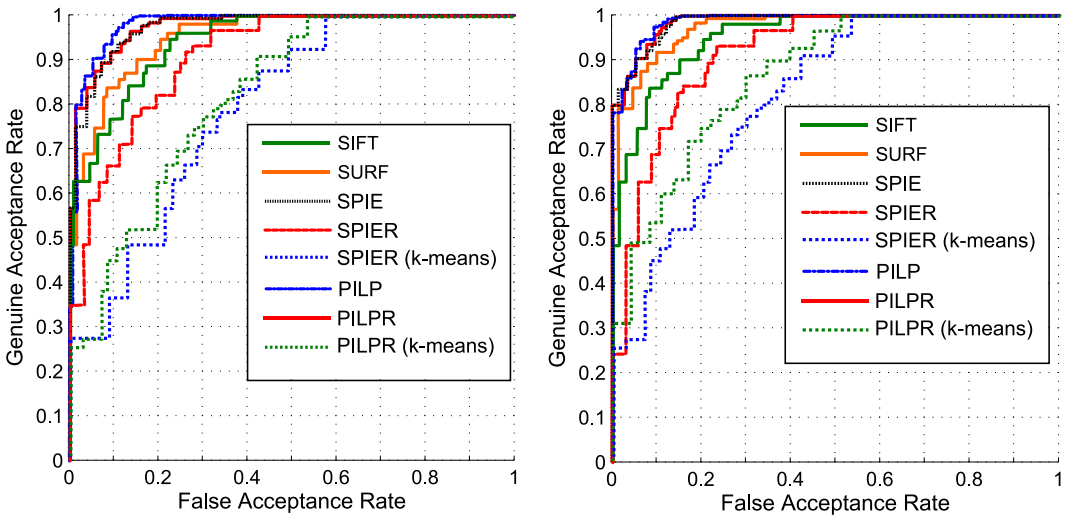

(a) BATH Database (b) CASIAv3 Database

Figure 3.12: ROC curve for various local features

3.4 Summary

In this chapter, feature reductions of SPIE and PILP are done using the suggested reduction scheme and studied. For both detectors, number of keypoints and time

Table 3.3: Performance of various local features

Databases →	BATH			CASIAv3		
Approaches ↓	ACC	FAR	FRR	ACC	FAR	FRR
SIFT	89.82	6.29	17.32	92.59	4.03	11.63
SURF	92.39	4.35	10.32	94.72	4.69	6.73
SPIE	94.23	3.48	7.69	96.33	2.85	5.23
SPIER	85.33	5.72	11.55	87.39	5.33	7.15
SPIER (k-means)	69.36	10.94	19.70	73.54	8.71	17.75
PILP	97.55	3.11	6.75	98.34	1.68	2.23
PILPR	96.23	2.39	4.63	97.68	1.25	1.96
PILPR (k-means)	72.31	9.45	18.24	76.63	7.56	15.81

Table 3.4: Time (in seconds) comparison for various local features

Databases →	BATH			CASIAv3		
Approaches ↓	Average #keypoints	Average time (extraction)	Average time (matching)	Average #keypoints	Average time (extraction)	Average time (matching)
SIFT	131.47	0.38	3.94	364.07	1.13	10.92
SURF	13.60	0.16	0.40	62.03	0.36	1.86
SPIE	10.23	1.53	0.36	54.74	4.93	1.64
SPIER	5.69	1.58	0.29	19.17	4.97	1.03
SPIER (k-means)	7.53	1.55	0.26	42.35	4.95	1.26
PILP	512.23	1.72	15.36	1526.55	5.17	45.79
PILPR	124.83	1.77	3.74	351.83	5.46	10.55
PILPR (k-means)	382.46	1.74	11.46	1141.89	5.28	33.64

reduced dramatically. However, the accuracy of reduced SPIE fell considerably as the number of decreased keypoints was too low. The suggested scheme applies density-based clustering to reduce the number of keypoints, and is found suitable for dense keypoint detector like PILP. Here, the number of keypoints and time reduced significantly, with a slight fall in accuracy. From the results it has been found that the average feature extraction time for the reduced PILP is 3.74 secs, which is roughly one-fifth of the actual PILP. The accuracy is found to be 96.23% for BATH and 97.68% for CASIAv3.

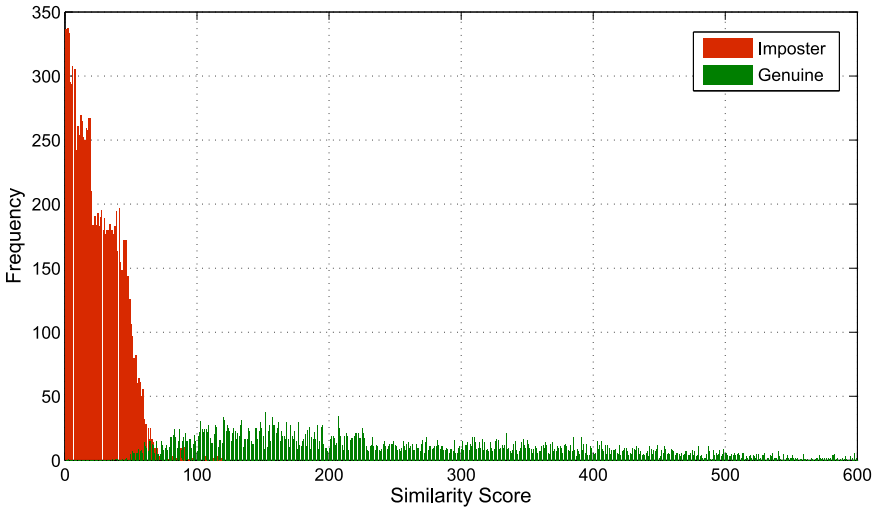

(a) BATH Database

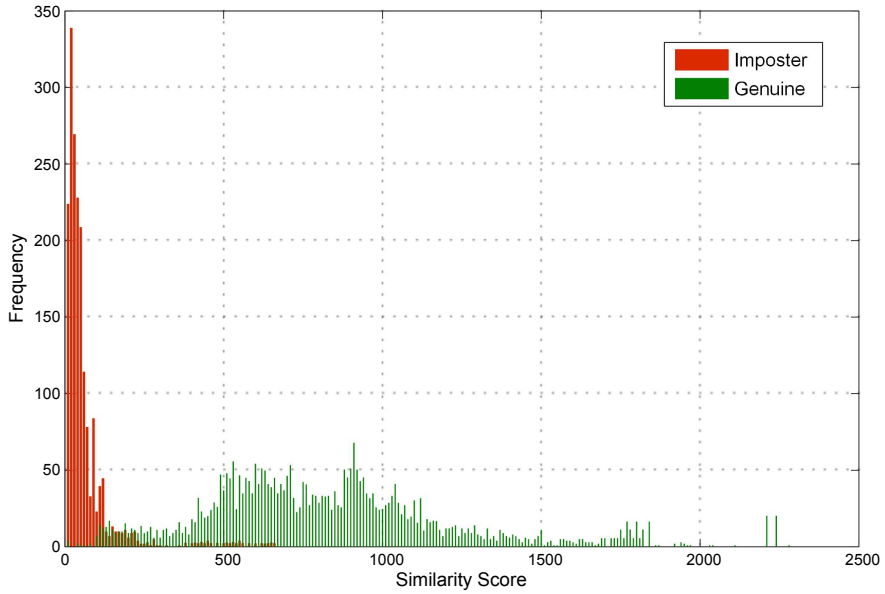

(b) CASIAv3 Database

Figure 3.13: Score distribution for reduced PILP

Chapter 4

Conclusions and Future Work

This thesis proposes two schemes; one for the keypoint detection and another for the keypoint reduction of the local features for iris biometrics. The first contribution deals with the salient keypoint detection using local entropy measures in the scale-space. Traditional local feature detectors consider corners as the point of interest; however, iris images are rich in texture. Thus salient points are the unpretentious choices for interest point detection. The proposed SPIE detector, identifies salient regions by measuring entropy of each points in the scale-space. Those points with higher entropy value in their neighborhood are considered as candidate keypoints. To evaluate its performance, experiments are conducted on the publicly available BATH and CASIAv3 iris databases, and their results are compared with the state-of-the-art SIFT and SURF features. The proposed method outperforms with achieving the overall accuracies of 94% and 96% for BATH and CASIAv3 databases respectively.

The second contribution is made to suggest a local feature reduction scheme in which an attempt is made to decrease the number of keypoints using clustering technique. The idea behind the proposed approach is to group the closely placed keypoints which are part of a larger feature and thereby reducing the number of keypoints. Density-based clustering (DBSCAN) is the most appropriate for such grouping situations. Initially, the keypoints are detected and are grouped using

DBSCAN. Each group of keypoints is then represented as a single keypoint for which an algorithm is also discussed. Keypoints are detected using the proposed SPIE detector; however, results are unsatisfactory. The main cause for this fall in performance is that the reduced number of keypoints is very low and loses its discriminative property. Therefore, the reduction scheme is quite appropriate for dense keypoint detector like PILP. It is capable of detecting large number of densely packed keypoints, giving an excellent recognition accuracy. Experiments are performed, and results prove that the suggested reduction scheme operates well with accuracies of 96% and 97% for BATH and CASIAv3 databases respectively. Additionally, there is a significant reduction in number of keypoints as well as computational time.

To conclude this thesis, the proposed schemes have been critically analyzed, and few limitations are noted. The proposed techniques involve the usage of existing state-of-the-art local descriptor like SIFT and SURF. Alternatively, a new descriptor can be designed using texture analysis, which would better describe the iris regions. Further, an efficient matching technique can be developed, using better data-structure like *kd*-tree or hashing techniques.

Bibliography

[1] T. Dunstone and N. Yager, *Biometric System and Data Analysis*. Springer, 2009.

[2] J. Wayman, A. Jain, D. Maltoni, and D. Maio, *Biometric Systems*. Springer, 2005.

[3] A. K. Jain, P. F. Ross, and A. Arun, *Handbook of Biometrics*. Springer, 2007.

[4] L. Flom and A. Safir, "Iris recognition system," US Patent 4 641 394, 1987.

[5] K. W. Bowyer, K. Hollingsworth, and P. J. Flynn, "Image understanding for iris biometrics: A survey," *Computer Vision and Image Understanding*, vol. 110, no. 2, pp. 281–307, 2008.

[6] D. G. Lowe, "Object recognition from local scale-invariant features," in *The proceedings of the Seventh IEEE International Conference on Computer Vision*, vol. 2, 1999, pp. 1150–1157.

[7] H. Bay, T. Tuytelaars, and L. V. Gool, "Speeded-up robust features (SURF)," *Computer Vision and Image Understanding*, vol. 110, no. 3, pp. 346–359, 2008.

[8] H. Mehrotra, G. Badrinath, B. Majhi, and P. Gupta, "An efficient iris recognition using local feature descriptor," in *16th IEEE International Conference on Image Processing (ICIP)*, Nov 2009, pp. 1957–1960.

[9] H. Mehrotra, B. Majhi, and P. Gupta, "Annular iris recognition using SURF," in *Pattern Recognition and Machine Intelligence*. Springer, 2009, pp. 464–469.

[10] K. Yang and E. Y. Du, "A multi-stage approach for non-cooperative iris recognition," in *IEEE International Conference on Systems, Man, and Cybernetics (SMC)*, Oct 2011, pp. 3386–3391.

[11] C. Belcher and Y. Du, "Region-based SIFT approach to iris recognition," *Optics and Lasers in Engineering*, vol. 47, no. 1, pp. 139–147, 2009.

[12] H. Mehrotra, P. K. Sa, and B. Majhi, "Fast segmentation and adaptive SURF descriptor for iris recognition," *Mathematical and Computer Modelling*, vol. 58, no. 1-2, pp. 132–146, 2013.

[13] C. Schmid, R. Mohr, and C. Bauckhage, "Evaluation of interest point detector," *International Journal of Computer Vision*, vol. 37, no. 2, pp. 151–172, 2000.

[14] S. Bakshi, P. K. Sa, and B. Majhi, "A novel phase-intensive local pattern for periocular recognition under visible spectrum," *Biocybernetics and Biomedical Engineering*, 2014, doi: 10.1016/j.bbe.2014.05.003.

[15] Bath University Database. [Online]. Available: http://www.bath.ac.uk/elec-eng/research/sipg/irisweb

[16] Chinese Academy of Sciences' Institute of Automation (CASIA) iris image database v3.0. [Online]. Available: http://www.cbsr.ia.ac.cn/english/IrisDatabase.asp

[17] M. Golfarelli, D. Maio, and D. Malton, "On the error-reject trade-off in biometric verification systems," *IEEE Transactions on Pattern Analysis and Machine Intelligence*, vol. 19, no. 7, pp. 786–796, 1997.

[18] J. Daugman, "High confidence visual recognition of persons by a test of statistical independence," *IEEE Transactions on Pattern Analysis and Machine Intelligence*, vol. 15, no. 11, pp. 1148–1161, 1993.

[19] R. Wildes, "Iris recognition: An emerging biometric technology," *Proceedings of the IEEE*, vol. 85, no. 9, pp. 1348–1363, 1997.

[20] W. Boles and B. Boashash, "A human identification technique using images of the iris and wavelet transform," *IEEE Transactions on Signal Processing*, vol. 46, no. 4, pp. 1185–1188, 1998.

[21] S. Lim, K. Lee, O. Byeon, and T. Kim, "Efficient iris recognition through improvement of feature vector and classifier," *ETRI Journal*, vol. 23, no. 2, pp. 61–70, 2001.

[22] L. Ma, T. Tan, Y. Wang, and D. Zhang, "Personal identification based on iris texture analysis," *IEEE Transactions on Pattern Analysis and Machine Intelligence*, vol. 25, no. 12, pp. 1519–1533, 2003.

[23] J. Daugman, "How iris recognition works?" *IEEE Transactions on Circuits and Systems for Video Technology*, vol. 14, no. 1, pp. 21–30, 2004.

[24] L. Ma, T. Tan, Y. Wang, and D. Zhang, "Efficient iris recognition by characterizing key local variations," *IEEE Transactions on Image Processing*, vol. 13, no. 6, pp. 739–750, 2004.

[25] D. Monro, S. Rakshit, and D. Zhang, "DCT-based iris recognition," *IEEE Transactions on Pattern Analysis and Machine Intelligence*, vol. 29, no. 4, pp. 586–595, 2007.

[26] H. Proenca and L. Alexandre, "Toward non-cooperative iris recognition: A classification approach using multiple signatures," *IEEE Transactions on Pattern Analysis and Machine Intelligence*, vol. 29, no. 4, pp. 607–612, 2007.

[27] M. Vatsa, R. Singh, and A. Noore, "Improving iris recognition performance using segmentation, quality enhancement, match score fusion, and indexing," *IEEE Transactions on Systems, Man, and Cybernetics, Part B: Cybernetics*, vol. 38, no. 4, pp. 1021–1035, 2008.

[28] M. Nabti and A. Bouridane, "An effective and fast iris recognition system based on a combined multiscale feature extraction technique," *Pattern Recognition*, vol. 41, no. 3, pp. 868–879, 2008.

[29] V. Velisavljevic, "Low-complexity iris coding and recognition based on directionlets," *IEEE Transactions on Information Forensics and Security*, vol. 4, no. 3, pp. 410–417, 2009.

[30] Z. Sun and T. Tan, "Ordinal measures for iris recognition," *IEEE Transactions on Pattern Analysis and Machine Intelligence*, vol. 31, no. 12, pp. 2211–2226, 2009.

[31] A. Abhyankar and S. Schuckers, "A novel biorthogonal wavelet network system for off-angle iris recognition," *Pattern Recognition*, vol. 43, no. 3, pp. 987–1007, 2010.

[32] J. Huang, X. You, Y. Yuan, F. Yang, and L. Lin, "Rotation invariant iris feature extraction using Gaussian Markov random fields with non-separable wavelet," *Neurocomputing*, vol. 73, no. 4-6, pp. 883–894, 2010.

[33] C. Chou, S.-W. Shih, W.-S. Chen, V. Cheng, and D.-Y. Chen, "Non-orthogonal view iris recognition system," *IEEE Transactions on Circuits and Systems for Video Technology*, vol. 20, no. 3, pp. 417–430, 2010.

[34] W. Dong, Z. Sun, and T. Tan, "Iris matching based on personalized weight map," *IEEE Transactions on Pattern Analysis and Machine Intelligence*, vol. 33, no. 9, pp. 1744–1757, 2011.

[35] A. Raffei, H. Asmuni, R. Hassan, and R. Othman, "Feature extraction for different distances of visible reflection iris using multiscale sparse representation of local Radon transform," *Pattern Recognition*, vol. 46, pp. 2622–2633, 2013.

[36] A. Rahulkar, L. Waghmare, and R. Holambe, "A new approach to the design of hybrid finer directional wavelet filter bank for iris feature extraction and classification using k-out-of-n: A post-classifier," *Pattern Analysis and Applications*, vol. 2013, pp. 1–19, 2013.

[37] N. K. Mahadeo, A. P. Paplinski, and S. Ray, "Optimization of iris codes for improved recognition," in *IEEE Conference on Computer Vision and Pattern Recognition Workshops (CVPRW)*, 2014, pp. 48–55.

[38] K. Popplewell, K. Roy, F. Ahmad, and J. Shelton, "Multispectral iris recognition utilizing hough transform and modified LBP," in *IEEE International Conference on Systems, Man and Cybernetics (SMC)*, 2014, pp. 1396–1399.

[39] D. G. Lowe, "Distinctive image features from scale-invariant keypoints," *International Journal of Computer Vision*, vol. 60, no. 2, pp. 91–110, 2004.

[40] H. P. Moravec, "Rover visual obstacle avoidance," in *International Joint Conference on Artificial Intelligence*, 1981, pp. 785–790.

[41] C. Harris and M. Stephens, "A combined corner and edge detector," in *Alvey Vision Conference*, vol. 15. Manchester, UK, 1988, p. 50.

[42] C. Harris, "Geometry from visual motion," in *Active vision*. MIT Press, 1993, pp. 263–284.

[43] T. Lindeberg, "Feature detection with automatic scale selection," *International Journal of Computer Vision*, vol. 30, no. 2, pp. 79–116, 1998.

[44] H. Xiao, W. He, K. Yuan, and F. Wen, "Real-time scene recognition on embedded system with SIFT keypoints and a new descriptor," in *IEEE International Conference on Mechatronics and Automation(ICMA)*, 2013, pp. 1317–1324.

[45] S. M. Smith and J. M. Brady, "SUSAN - a new approach to low level image processing," *International Journal of Computer Vision*, vol. 23, no. 1, pp. 45–78, 1997.

[46] K. Mikolajczyk and C. Schmid, "Scale & affine invariant interest point detectors," *International Journal of Computer Vision*, vol. 60, no. 1, pp. 63–86, 2004.

[47] T. Kadir, A. Zisserman, and M. Brady, "An affine invariant salient region detector," in *Computer Vision-ECCV 2004*. Springer, 2004, pp. 228–241.

[48] E. Rosten and T. Drummond, "Machine learning for high-speed corner detection," in *Computer Vision–ECCV 2006*. Springer, 2006, pp. 430–443.

[49] M. Agrawal, K. Konolige, and M. R. Blas, "CenSurE: Center surround extremas for realtime feature detection and matching," in *Computer Vision–ECCV*. Springer, 2008, pp. 102–115.

[50] M. Ebrahimi and W. W. Mayol-Cuevas, "SUSurE: Speeded up surround extrema feature detector and descriptor for realtime applications," in *IEEE Computer Society Conference on Computer Vision and Pattern Recognition Workshops (CVPRW)*, 2009, pp. 9–14.

[51] E. Mair, G. D. Hager, D. Burschka, M. Suppa, and G. Hirzinger, "Adaptive and generic corner detection based on the accelerated segment test," in *Computer Vision–ECCV*. Springer, 2010, pp. 183–196.

[52] S. Leutenegger, M. Chli, and R. Y. Siegwart, "BRISK: Binary robust invariant scalable keypoints," in *IEEE International Conference on Computer Vision (ICCV)*, 2011, pp. 2548–2555.

[53] S. Gilles, "Robust description and matching of images," in *University of Oxford*, 1999.

[54] C. Schmid and R. Mohr, "Local grayvalue invariants for image retrieval," *IEEE Transactions on Pattern Analysis and Machine Intelligence*, vol. 19, no. 5, pp. 530–534, 1997.

[55] B. Schiele and J. L. Crowley, "Object recognition using multidimensional receptive field histograms," in *European Conference on Computer Vision (ECCV)*. Springer, 1996, pp. 610–619.

[56] M. J. Swain and D. H. Ballard, "Color indexing," *International Journal of Computer Vision*, vol. 7, no. 1, pp. 11–32, 1991.

[57] T. Lindeberg, "Scale-space theory: A basic tool for analyzing structures at different scales," *Journal of Applied Statistics*, vol. 21, no. 1-2, pp. 225–270, 1994.

[58] C. E. Shannon, "A mathematical theory of communication," *ACM SIGMOBILE Mobile Computing and Communications Review*, vol. 5, no. 1, pp. 3–55, 2001.

[59] Y. Ke and R. Sukthankar, "PCA-SIFT: A more distinctive representation for local image descriptors," in *IEEE Computer Society Conference on Computer Vision and Pattern Recognition (CVPR)*, vol. 2, 2004, pp. 506–513.

[60] G. Hua, M. Brown, and S. Winder, "Discriminant embedding for local image descriptors," in *IEEE 11th International Conference on Computer Vision*, 2007, pp. 1–8.

[61] R. J. Alitappeh, K. J. Saravi, and F. Mahmoudi, "Key point reduction in SIFT descriptor used by subtractive clustering," in *11th International Conference on Information Science, Signal Processing and their Applications (ISSPA)*, 2012, pp. 906–911.

[62] M. Rudinac, B. Lenseigne, and P. Jonker, "Entropy based method for keypoint selection," in *Fifteenth Annual Conference of the Advanced School for Computing and Imaging*, 2009.

[63] K. Yuasa and T. Wada, "Keypoint reduction for smart image retrieval," in *IEEE International Symposium on Multimedia (ISM)*, 2013, pp. 351–358.

[64] M. Ester, H.-P. Kriegel, J. Sander, and X. Xu, "A density-based algorithm for discovering clusters in large spatial databases with noise." in *Second International Conference on Knowledge Discovery and Data Mining (KDD)*, vol. 96. AAAI Press, 1996, pp. 226–231.

[65] T. Lindeberg and L. Bretzner, "Real-time scale selection in hybrid multi-scale representations," in *Scale Space Methods in Computer Vision*. Springer, 2003, pp. 148–163.

Dissemination

- Beeren Sahu, Banshidhar Majhi and Pankaj K. Sa, "Salient Keypoint Detection using Entropy Map for Iris Biometrics," *2nd International Conference on Perception and Machine Intelligence (PerMin - Kolkata)*, ACM, February 2015, doi: 10.1145/2708463.2709052.

Index